This is a preprint, the final version is subject to change, of the American Mineralogist (MSA)
Cite as Authors (Year) Title. American Mineralogist, in press.
(DOI will not work until issue is live.) DOI: http://dx.doi.org/10.2138/am-2017-5724

Revision #2

Geochemical and radiogenic isotope probes of Ischia volcano, Southern Italy: constraints on magma chamber dynamics and residence time

Martina Casalini[1,2], Riccardo Avanzinelli[1], Arnd Heumann[3], Sandro de Vita[4], Fabio Sansivero[4], Sandro Conticelli[1,5], Simone Tommasini[1,*]

1. Dipartimento di Scienze della Terra, Università degli Studi di Firenze, via G. La Pira 4, Firenze, Italy

2. Dipartimento di Scienze della Terra, Università degli Studi di Pisa, via Santa Maria 53, Pisa, Italy

3. GFZ German Research Centre for Geosciences, Telegrafenberg, 14473 Potsdam, Germany

4. Istituto Nazionale di Geofisica e Vulcanologia, Sezione di Napoli Osservatorio Vesuviano, via Diocleziano 328, Napoli, Italy

5. U.O.S. di Firenze, Istituto di Geoscienze e Georisorse, Consiglio Nazionale delle Ricerche, via G. La Pira 4, Firenze, Italy

* corresponding author: simone.tommasini@unifi.it

Always consult and cite the final, published document. See http:/www.minsocam.org or GeoscienceWorld

Abstract

The active volcano of Ischia, an island off-shore the city of Naples, Southern Italy, has a discontinuous volcanic activity characterized by caldera-forming paroxysmal eruptions, lava flows, and lava domes, and thus offers the opportunity to study the complexity of magma storage, differentiation, and extraction mechanisms in a long-lived magma reservoir. The overall geochemical composition of erupted magmas varies from shoshonite to latite and trachyte/trachyphonolite. Their Sr and Nd, isotope composition variation is typical of subduction-related magmas, akin to other potassic magmas of the Neapolitan District, and there is a complete overlap of radiogenic isotope composition among shoshonite, latite, and trachyte/trachyphonolite. The lack of systematic radiogenic isotope covariation during differentiation suggests that the radiogenic isotope variability could be a signature of each magma pulse that subsequently evolved in a closed-system environment. Erupted magmas record a recurrent evolutionary process consisting of two-step fractional crystallization along similar liquid lines of descent for each magma pulse, suggesting near steady-state magma chamber conditions with balanced alternating periods of replenishment, differentiation, and eruption. The dominant role of fractionating feldspars determines a significant depletion of Sr (<10 ppm) coupled with high Rb/Sr (>200) in the residual trachyte magma.

A number of more-evolved trachytes have anomalously radiogenic $^{87}Sr/^{86}Sr_i$ (>0.707) coupled with high $^{87}Rb/^{86}Sr$ (>50), all other geochemical and isotopic characteristics being similar to normal $^{87}Sr/^{86}Sr_i$ trachytes at the same degree of evolution. This radiogenic Sr isotope signature is not consistent with assimilation of crustal material and demands for a time-related in-growth of ^{87}Sr during storage within the magma chamber. Rb-Sr isochrons on separated mineral-groundmass pairs provide robust constraints on a prolonged pre-eruptive history ranging from a few tens to hundreds of thousands of years at relatively low temperature (~750°C). Remarkably, also normal trachytes with high $^{87}Rb/^{86}Sr$ (>200) yield a magma residence time from some 4 to 27 kyr, implying that the

Always consult and cite the final, published document. See http:/www.minsocam.org or GeoscienceWorld

This is a preprint, the final version is subject to change, of the American Mineralogist (MSA)
Cite as Authors (Year) Title. American Mineralogist, in press.
(DOI will not work until issue is live.) DOI: http://dx.doi.org/10.2138/am-2017-5724

long-lived history of Ischia magmas is not limited to the anomalous $^{87}Sr/^{86}Sr_i$ trachytes. This long-lived history could be a characteristic feature of the magma chamber reservoir of this active volcano, which other volcanic products (i.e., shoshonite and latite) cannot disclose due to their lower Rb/Sr (i.e., low ^{87}Sr in-growth rate) and higher magma storage temperature (>900°C) (i.e., rapid Sr isotope homogenization via diffusion).

The magma chamber dynamics of the active volcano of Ischia, probed on the basis of geochemical and radiogenic isotope tools, is consistent with recent models of complex magma chamber reservoirs made up of multiple discrete melt pockets, isolated by largely crystalline mush portions, maintained in a steady-state thermal flux regime with no mass exchange, and with reactivation shortly before eruption.

Keywords: Ischia volcano, radiogenic isotopes, geochemistry, magma chamber dynamics, magma residence time

Introduction

The largest and most destructive eruptions on Earth are often characterized by the eruption of highly differentiated magma. Melt enrichment in volatile elements due to differentiation processes changes the rheology of magma and provides favourable conditions for paroxysmal eruptions depending upon magma residence time along with magma chamber geometries and dynamics (e.g, Huppert & Woods, 2002; Francalanci et al., 2005; Bachmann & Bergantz, 2008a; Braschi et al., 2012; Conticelli et al., 2015a). Understanding the rate at which magma differentiates and how long magma resides in the magmatic system, is key for volcanological studies. Important constraints come from the “crystal-mush model” (Hildreth, 2004; Bachman & Bergantz, 2004, 2008a, 2008b; Marsh, 2006), suggesting that a significant mass fraction of magma resides within large bodies of crystal-rich zones of broadly intermediate bulk composition with highly-silicic interstitial melt. Cooper & Kent (2014) have also proposed that magmas can be stored at relatively low temperature

Always consult and cite the final, published document. See http:/www.minsocam.org or GeoscienceWorld

(inhibiting diffusion but not radioactive decay) for long periods of time, to be reactivated shortly before the eruption.

In this context, a recent model (Cashman & Giordano, 2014) suggests that large magma reservoirs are made up of isolated pockets or lenses of melt separated by the presence of rigid or impermeable crystal mushes, along with physical and/or rheological barriers (e.g., Stroncik et al., 2009; Barker et al., 2015). These individual pockets can be tapped and erupted together (simultaneously or in succession) during major eruptions without significant physical and chemical homogenization. Such a new model is rapidly gaining consensus among the volcanological community (e.g., Ellis et al., 2014; Alloway et al., 2015; Barker et al., 2015; Tibaldi 2015; Willcock et al., 2015) and would have crucial implications on the mechanism of melt extraction and the duration of explosive volcanic eruptions in terms of prolonged maintenance and/or fluctuations of excess pressure (Gudmundsson, 2012). Either direct or indirect evidence supporting (or contradicting) this new model, however, has proved difficult to obtain from classical geological, geophysical or geochemical data (e.g., Cashman & Giordano, 2014).

The focus of our study is on the active volcano of Ischia, which forms one out of four volcanic complexes of the Neapolitan District (e.g., Conticelli et al 2015b, and references therein), Southern Italy (Fig. 1 inset). The Ischia volcano offers the opportunity to investigate conditions of magma storage, differentiation, and extraction mechanisms in complex magma reservoirs because of its recent volcanic activity (from <150 ka to 1302 AD), which has been characterized by discontinuous highly explosive and effusive phases separated by long periods of quiescence (e.g., Gillot et al. 1982; Vezzoli 1988; Orsi et al. 1996; de Vita et al. 2006, 2010; Brown et al., 2008). Despite a number of different models that were suggested to explain the overall magma evolution, there is a general consensus that fractional crystallization, magma mixing/mingling, and assimilation of continental crust in an open system control the evolution and the geochemical and isotopic variations of Ischia magmas (e.g., Poli et al., 1987, 1989; Crisci et al., 1989; Civetta et al.,

Always consult and cite the final, published document. See http:/www.minsocam.org or GeoscienceWorld

1991; Di Girolamo et al., 1995; Piochi et al., 1999); D'Antonio et al., 2007, 2013; Brown et al., 2014; Melluso et al., 2014). In this paper we report a comprehensive major, trace elements and radiogenic isotopes (Sr, Nd) dataset of unpublished whole rock data, to discuss the differentiation processes occurring at Ischia and their timescales. We further test our interpretation with new Rb-Sr isochron data on mineral and groundmass separates, providing new insights into the temporal relationships of melt storage underneath the Ischia magmatic reservoir.

Volcanological Background

The active volcanoes of Ischia, Procida, Phlegrean Fields, and Somma-Vesuvius, belong to the Neapolitan District (Fig. 1 inset) and form the southernmost cluster of volcanoes of the Roman Magmatic Province (e.g., Washington, 1906; Conticelli et al., 2004, 2010, 2015b; Peccerillo, 2005; Avanzinelli et al., 2009). The island of Ischia is the remnant of a larger volcanic edifice located at the northwestern corner of the Gulf of Naples (Fig. 1 inset). The subaerial portion of the Ischia volcano (~46 km^2) is composed of pyroclastic rocks with minor lava flows and domes, landslide deposits, and terrigenous sedimentary rocks (de Vita et al., 2006; 2010; Della Seta et al., 2012, and references therein). The morphology of the island reflects a complex history of alternating constructive and destructive phases, due to the interplay among tectonics, volcanic activity, and gravitational surface movements (e.g., Vezzoli, 1988; Orsi et al., 1991; 2003; Acocella and Funiciello, 1999; Acocella et al., 2001; 2004; de Vita et al., 2006, 2010; Della Seta et al., 2012). The subaerial volcanic activity of Ischia has been divided into five main phases (Fig. 1) on the basis of radiometric ages, and stratigraphic, geochemical, and radiogenic isotope data (e.g., Gillot et al., 1982; Poli et al., 1987, 1989; Vezzoli, 1988; Crisci et al., 1989; Civetta et al., 1991; Tibaldi and Vezzoli, 2004; Brown et al., 2008, 2014; Melluso et al., 2014).

I Phase – the oldest outcropping phase of subaerial volcanic activity occurred between 150 and 75 ka BP with eruption of mainly trachytic and trachyphonolitic lava flows and domes, along

Always consult and cite the final, published document. See http:/www.minsocam.org or GeoscienceWorld

with minor pyroclastic rocks (e.g., Gillot et al., 1982; Vezzoli, 1988; Crisci et al., 1989; Brown et al., 2014; Melluso et al., 2014). The volcanic rocks of the first phase outcrop discontinuously along the southernmost shoreline of the island, from Punta Imperatore to Punta San Pancrazio, and in scattered outcrops along the periphery of the island (Fig. 1).

II Phase – the second phase occurred between 75 and 55 ka BP, and was marked by a change of the eruptive style from mainly effusive to highly explosive eruptions with emplacement of complex successions of trachytic pumice falls interlayered with pyroclastic density currents and breccias (Orsi et al., 1991; Brown et al., 2008). The volcanic rocks of this phase outcrop continuously along the southeastern sector of the island overlaying the rocks of the I Cycle (Fig. 1).

III Phase – the third phase occurred between 55 ka and 33 ka BP, and commenced with the paroxysmal Mt. Epomeo Green Tuff eruption, forming a ~10x7 km caldera and erupting some 40 km^3 of volcanic products (e.g., Vezzoli, 1988; Tibaldi and Vezzoli, 1998, Tomlinson et al., 2014). The Mt. Epomeo Green Tuff consists of trachytic ignimbrites partially filling a submerged depression, which now makes up the central part of the island (Fig. 1). Minor trachytic hydromagmatic to magmatic eruptions from small vents along the southwestern and northwestern sectors of the island (Fig. 1) prolonged this phase up to 33 ka (de Vita et al., 2010).

IV Phase – volcanic activity renewed at 28 ka, after 5 kyr of quiescence, with the arrival of shoshonitic magma into the main reservoir, which triggered the Mt. Epomeo caldera resurgence of some 900 m (Poli et al., 1989, Civetta et al., 1991 Orsi et al., 1991, de Vita et al., 2006). This phase continued sporadically with mild explosive and effusive eruptions until 18 ka BP, and its products are scattered along the peripheral sector of the island, at Mt. Vico, between Punta Imperatore and Mt. St. Angelo, and south of Castello (Fig. 1).

V Phase - the last phase of activity commenced at about 10 ka and is still active with the last historic lava flow eruption recorded at Mt. Arso in 1302 AD (de Vita et al., 2010, and references therein). This phase is characterized by mainly latitic to trachytic monogenetic volcanic activity and

Always consult and cite the final, published document. See http:/www.minsocam.org or GeoscienceWorld

ongoing Mt. Epomeo caldera resurgence (e.g., Orsi et al., 1991, 1996; Buchner et al., 1996; de Vita et al., 2006, 2010). Caldera resurgence restricted eruptions to the eastern sector of the island with only a few vents located outside this sector, along regional fault systems. The volcanic activity was characterized by lava domes and high-aspect ratio lava flows, together with magmatic and phreatomagmatic explosive eruptions that generated tuff-cones, tuff-rings and variably dispersed pyroclastic fall and pyroclastic current deposits (de Vita et al., 2010, and references therein).

A historical record of earthquakes (e.g., the 1883 Casamicciola earthquake, Cubellis et al., 2004), historical ground movements (Buchner et al., 1996; de Vita et al., 2006; Della Seta et al., 2012), fumaroles and thermal springs (Inguaggiato et al., 2000; Chiodini et al., 2004; Di Napoli et al., 2011) complements the present day activity.

Analytical techniques

Major and trace elements have been analysed by ICP-AES and ICP-MS at Activation Laboratories Ltd. (Ancaster, Ontario, see http://www.actlabs.com for details). Mineral separation has been carried out at the IGG-CNR of Pisa, whilst Sr and Nd isotope measurements have been performed by magnetic sector multi-collector Thermofisher Triton-Ti mass spectrometer at the Earth Science Department of the Università degli Studi di Firenze. Rb-Sr isotope dilution and isotope composition analyses have been performed on selected samples from single sample dissolution and subsequent splitting (20% solution for isotope dilution and 80% solution for isotope composition) using a mixed ^{84}Sr -^{87}Rb spike and then analysed by the Thermofisher Triton-Ti mass spectrometer at the Earth Science Department of the Università degli Studi di Firenze.

The selected samples for isotope dilution have been crushed and then sieved at different particle size diameters. Enriched fractions of sanidine, clinopyroxene (300 and 250 μm), and glass/groundmass (150 and 100 μm) were obtained by a Frantz isodynamic separator. Each separated fraction has been handpicked under a binocular microscope to obtain >95 % purity. The

Always consult and cite the final, published document. See http:/www.minsocam.org or GeoscienceWorld

clinopyroxene has been separated only from the sample having this phase as microphenocryst (ISC10-01). After leaching with warm (50°C) 1N HCl for 1 hour in ultrasonic bath, and rinsing with Milli-Q water, mineral separates and whole-rock samples were dissolved in 15 ml Savillex PFA beakers in a HF-HNO_3-HCl mixture. Rb-Sr, and Nd purification has been carried out using standard chromatographic techniques (e.g., Avanzinelli et al., 2005).

Sr and Nd isotopes were measured in dynamic mode (Avanzinelli et al., 2005) and the effect of mass fractionation has been corrected using an exponential law to $^{86}Sr/^{88}Sr$= 0.1194 and $^{146}Nd/^{144}Nd$= 0.7219, respectively. All errors reported are within run precision ($2\sigma_m$), and are typically <10 ppm. Repeated analyses of the NIST SRM 987 and a Nd internal standard (Nd-Fi) yielded $^{87}Sr/^{86}Sr$= 0.710249±11 (2σ, n= 23), and $^{143}Nd/^{144}Nd$= 0.511467±8 (2σ, n= 15) over the period of analyses. The Nd isotope composition of the internal standard Nd-Fi is referred to the La Jolla $^{143}Nd/^{144}Nd$= 0.511847±7 (2σ, n= 53) measured in our laboratory. Rb-Sr isotope dilution analyses were performed in static mode and the effect of mass fractionation has been corrected using an exponential law to $^{86}Sr/^{88}Sr$= 0.1194 and a factor of 2.8 ‰ per amu for Rb on the basis of repeated analyses of the Rb standard Romil ($^{85}Rb/^{87}Rb$ = 2.6071±18, 2σ, n= 12). Total procedural blanks were <290 pg (Sr), <120 pg (Nd), and required no correction to the samples.

Results

Petrographic characteristics

A total of fresh 38 rock samples (supplementary Table S1) have been collected along well-established volcanic log sequences in order to represent the whole spectrum of magmas erupted during the five phases of subaerial volcanic activity at Ischia and provide geochemical arguments on differentiation processes, and magma storage timescales. Among these, four samples have been further selected for mineral separation and Rb-Sr isotope dilution analyses, on the basis of their whole-rock Sr isotope composition and high Rb/Sr.

Always consult and cite the final, published document. See http:/www.minsocam.org or GeoscienceWorld

The two shoshonite and latite samples are from the V Phase of volcanic activity and represent the Arso lava flow and the Molara scoria cone (Fig. 1). One latite sample is a mafic enclave within the Zaro lava flow (Fig. 1). The other samples are all trachytes and trachytes/phonolites lava flows, domes, and pumices covering the five phases of volcanic activity at Ischia (supplementary Table S1).

Shoshonites and latites are porphyritic lavas with sanidine, plagioclase, clinopyroxene phenocrysts in a very fine-grained groundmass made up of feldspar laths, clinopyroxene, biotite, olivine, and magnetite. The mafic enclave within the Zaro lava flow has a porphyritic texture with phenocrysts of olivine, plagioclase and clinopyroxene in a microcrystalline groundmass made up of feldspar, clinopyroxene, olivine, biotite, and magnetite. Trachytes and trachytes/phonolites have a porphyritic texture and are characterized by sanidine phenocrysts, up to 10 mm in elongation, in a micro- crypto-crystalline (lava flow and dome) to hyaline (pumice) groundmass composed of feldspar laths, biotite, clinopyroxene, and glass, with accessory magnetite, sphene, and apatite. Fluidal alignment of sanidine laths in the groundmass confers the typical trachytic texture to the rocks. The overall petrographic characteristics of the studied samples are consistent with previous studies on the same volcanic log sequences (e.g., Civetta et al., 1991; Di Girolamo et al., 1995; D'Antonio et al., 2013; Brown et al., 2014; Melluso et al., 2014, and references therein)

Major and trace elements

Major and trace element data, along with Sr and Nd radiogenic isotope compositions of the 38 unpublished whole rock samples are reported in Supplementary Table S2, and Table 1, respectively. Ischia volcanic rocks have potassic affinity ($Na_2O - 2 \leq K_2O$, Le Maitre et al., 1989), and belong to the shoshonitic series within the Neapolitan District of the Roman Magmatic Province (i.e., KS or low-K series, Appleton, 1972; Conticelli et al., 2010; D'Antonio et al., 2013). The major element composition of the studied magmas at Ischia varies from shoshonite to latite, trachyte, and phonolite

Always consult and cite the final, published document. See http:/www.minsocam.org or GeoscienceWorld

(Fig. 2), and cover the whole spectrum of composition reported in the literature (e.g., Poli et al., 1987; Civetta et al., 1991; Conticelli et al., 2010; Brown et al., 2014; Melluso et al., 2014, and references therein). Most of the samples collected in this study straddle the trachyte-phonolite boundary (hereafter trachyte as a whole), with minor latites and shoshonites (Fig. 2)

The geochemical evolution of Ischia magmas from shoshonite through latite, and trachyte is characterized by an abrupt compositional variation of the liquid line of descent at ~2 wt% CaO (e.g., Fig. 3), as previously outlined by Brown et al. (2014). Magma compositional variation from shoshonite (CaO ~7 wt) to trachyte (CaO ~2 wt%) exhibits a decrease in MgO, FeO, TiO_2, and P_2O_5 coupled with an increase in SiO_2, K_2O, and Na_2O, and constant Al_2O_3. Magma compositional variation within trachyte (CaO from ~2 wt% to ~0.8 wt%) continues along the same liquid line of descent for all major elements but K_2O that exhibits a significant decrease (Fig. 3a). Incompatible trace elements (High Field Strength Elements, Rare Earth Elements, and most Large Ion Litophile Elements) have a smooth increase from ~7 wt.% to ~2 wt% CaO, and then a rapid two- three-fold increase from ~2 wt.% to ~0.8 wt% CaO (e.g., La, Fig. 3b), whilst transition metals, Sr, and Ba show a positive and continuous correlation with CaO (e.g., Sr, Fig. 3c). The same compositional variation of the liquid line of descent can be observed also using trace elements as differentiation index. For example, Rb/Sr increases from ~0.3 to ~3.3, from shoshonite to trachyte, and then reaches values as high as 230 with proceeding trachyte evolution owing to the drastic decrease of Sr content (Fig. 4a). Light REE fractionation has a smooth increase from ~240 ppm to ~30 ppm V, followed by a rapid three-fold increase at almost constant V content (Fig. 4b). Current estimates of temperature decrease with magma evolution (Fig. 4a) yield 880-1030 °C for a mafic inclusion within the Zaro shoshonite (Sr ~500 ppm), and 700-770°C for a trachyte from Castello (Sr ~10 ppm) on the basis of titaniferous magnetite-melt equilibria (Melluso et al., 2014). Brown et al. (2014) reported a temperature of 930°C for another trachyte (Sr ~100 ppm) based on both MELTS (Gualda et al., 2012) calculation and biotite-melt equilibrium.

Always consult and cite the final, published document. See http:/www.minsocam.org or GeoscienceWorld

Radiogenic isotopes

The Ischia volcanic rocks have Sr and Nd isotope compositions transitional between those of Procida and Somma Vesuvio within the Neapolitan District (Fig. 5) (e.g., Civetta et al., 1991; Piochi et al., 1999; D'Antonio et al., 1999, 2007, 2013; Conticelli et al., 2002, 2010, 2015b; Avanzinelli et al., 2008, 2009). In terms of Sr and Nd isotope composition, Ischia magmas exhibit a complete overlap among shoshonite, latite, and trachyte (Fig. 5), with no systematic variation between more-evolved and less-evolved magmas. The overall radiogenic isotope composition is similar to that of typical subduction related magmas (e.g., Elliott, 2003), with negative correlation between $^{143}Nd/^{144}Nd$ *vs.* $^{87}Sr/^{86}Sr$ (Fig. 5). In this context, the radiogenic isotope composition of Ischia magmas is consistent with the mantle source heterogeneity recorded as a whole by the potassic and ultrapotassic magmas of the Roman Magmatic Province, in particular those of the Neapolitan District (Fig. 5), pointing to variable addition of crustal components to the mantle wedge through the subduction process related to the Apennine orogeny (e.g., Crisci et al., 1989; Beccaluva et al., 1991; Conticelli and Peccerillo, 1992; D'Antonio et al., 1999, 2013; Peccerillo, 1999, 2001, 2005; Conticelli et al., 2002, 2009, 2010, 2015b; Avanzinelli et al., 2008, 2009; Moretti et al., 2013; Mazzeo et al., 2014).

A notable exception to the general co-variation between the different radiogenic isotope compositions is represented by a number of highly-evolved trachytes with $^{87}Sr/^{86}Sr_i>0.707$. Despite their anomalous $^{87}Sr/^{86}Sr_i$, these samples have Nd isotope compositions overlapping with other samples (Fig. 5). The other striking characteristics of such anomalous samples are (i) the invariably low Sr content (<34 ppm, Table S2, Fig. 4), (ii)the high Rb/Sr (from 13 to 230, Table S2, Fig. 4), and (iii) the evolution along a liquid line of descent indistinguishable from that of other trachytes (Figs. 3, 4). Trachytes with high radiogenic Sr isotopes have been reported also by Poli et al.

Always consult and cite the final, published document. See http:/www.minsocam.org or GeoscienceWorld

(1987), although these authors do not provide Nd isotope composition and do not discuss them in details.

Temporal evolution

Considering the temporal variation of erupted magmas over the past 150 kyr of volcanic activity at Ischia (Fig. 6a), the recurrence of more- and less-evolved products (using CaO as a *proxy*, Fig. 3) is indicative of alternating periods of replenishment, differentiation, eruption, and quiescence in a dynamic volcanic system (e.g., Poli et al., 1989; Civetta et al., 1991; de Vita et al., 2010; D'Antonio et al., 2013; Brown et al., 2014).

More-evolved compositions (i.e., trachytes) are more common in the volcanic products preceding the Mt. Epomeo eruption at 55 ka, whilst in the most recent phases of activity the erupted magmas have a more variable composition including both more- and less-evolved products (Fig. 6a). Actual volume estimates or erupted volcanic product are, however, difficult to ascertain because of the lack of studies focused on the amount of erupted material during each eruptive phase. Tentatively, the reason of such a time-dependent distribution of erupted magmas could be simply due to an outcrop bias, i.e. shoshonite and latite eruptions of the older phases of activity are masked by products of the subsequent eruptive phases. Alternatively, the absence of shoshonite and latite in the oldest periods of activity could be due to a change in the eruptive style following the paroxysmal Mt. Epomeo eruption. This would mean that before 55 ka the volcanic system had an obstructed system of channels feeding the volcanic vents, allowing sufficient time to drive magma evolution and differentiation. Following the Mt. Epomeo eruption, due to the interplay between regional tectonics and volcanic activity (i.e. Mt. Epomeo block resurgence, Marotta and de Vita, 2014, and references therein), the system of channels feeding the volcanic vents may have become less obstructed than in the previous volcanic history, allowing the eruption of less differentiated

Always consult and cite the final, published document. See http:/www.minsocam.org or GeoscienceWorld

magmas, in the form of lava flows and lava domes, shortly after their arrival in the magma chamber without sufficient time for differentiation processes to operate.

The time-series Sr and Nd isotope composition of erupted magmas clearly shows that both more- and less-evolved magmas have similar radiogenic isotope signatures in each activity phase (Fig. 6b, c). The Sr isotope compositions of erupted magmas as a whole, except the highly-evolved trachytes with $^{87}Sr/^{86}Sr_i$>0.707, define a sort of smooth sinusoidal variation curve with the least and the most radiogenic magmas erupted at ca. 6 ka and 55 ka, respectively. In the last 10 kyr, there is a slight trend towards Sr isotope composition similar to those of the I Phase (Fig. 6b). The variation of Nd isotope composition through time is less discernible than Sr isotopes (Fig. 6c), and, remarkably, the highly-evolved trachytes with $^{87}Sr/^{86}Sr_i$>0.707 have the same Nd isotope composition as other more- and less-evolved magmas of the corresponding activity phase. The sample with the most radiogenic Nd and unradiogenic Sr isotope composition is a mafic enclave within Zaro lava flow (Table 1). It is noteworthy that despite the Sr and Nd isotope variation, each magma pulse over the past 150 kyr evolved and differentiated along similar liquid lines of descent (Figs. 3, 4), suggestive of a steady-state volcanic system in term of fractionating mineral assemblage, independent upon age.

Discussion

Understanding magma chamber dynamics related to the long term evolution of magmas and the transition from highly explosive to effusive eruptions, is key to the volcanological study of Ischia, since large caldera-forming eruptions typically have long repose periods (10^3-10^5 yr, e.g., Cashman & Giordano, 2014). Previous studies (e.g., Crisci et al., 1989; D'Antonio et al., 2013; Brown et al., 2014; Melluso et al., 2014, and references therein) have demonstrated that the overall geochemical evolution of Ischia magmas, from shoshonite through latite and trachyte, can be modelled as a two-step fractional crystallization process on the basis of the abrupt compositional

Always consult and cite the final, published document. See http:/www.minsocam.org or GeoscienceWorld

variation of the liquid line of descent at ~2 wt% CaO (e.g., Fig. 3). The kink at 2 wt% CaO has been taken as evidence of changing the fractionating mineral assemblage. The first step is characterized by crystallization of olivine + plagioclase + clinopyroxene + Fe-Ti oxides + biotite + apatite, driving the magma composition from shoshonite (CaO ~7 wt%) to trachyte (CaO ~2 wt%). The second step, responsible for producing the most differentiated trachytic compositions (CaO <2 wt%) is dominated by crystallization of sanidine, as indicated by the sudden decrease in K_2O (Fig. 3a), with minor plagioclase + clinopyroxene + apatite.

Our new whole rock data are consistent with the two-step fractional crystallization process, which remained constant over the past 150 kyr, with all samples evolving along similar liquid lines of descent (Figs. 3, 4). The extreme enrichment of incompatible trace elements during the second step (e.g., threefold for La, Fig. 3b) is caused, in addition to changing the fractionating mineral assemblage, by the significant increase of the enrichment factor (Cl/C_0) as the fraction of residual liquid vanishes. The extreme Sr content depletion and Rb/Sr increase (Fig. 4a) is caused by the major role of feldspars (first step: plagioclase, second step: sanidine) during magma differentiation (e.g., Halliday et al., 1991).

In addition to the closed system crystal fractionation process, the observed radiogenic isotope variation of less-evolved magmas belonging to the first step (blue circles, Fig. 5) has been attributed to contamination by Hercynian crust of the distinct magma batches feeding the Ischia magma chamber (e.g., Brown et al., 2014). The variation of Sr isotopes *vs* Sr content (Fig. 7) is difficult to reconcile with contamination processes starting from a single parental magma composition. The $^{87}Sr/^{86}Sr_i$ spread of magmas at the highest Sr content (some 500-600 ppm), is identical to that observed at low Sr content (Fig. 7), implying that there is no systematic $^{87}Sr/^{86}Sr$ increase with proceeding evolution as would be expected in case of contamination processes by radiogenic crustal material. A similar correlation between Sr isotopes and indices of magma differentiations (e.g., Fig. 7) would be expected in the case of mixing between more- and less- evolved magmas with different

Always consult and cite the final, published document. See http:/www.minsocam.org or GeoscienceWorld

isotope compositions. Therefore, the observed isotope variability can derive from either original differences of the parental magmas, which do not outcrop on the island, or to more complex contamination processes affecting, independently, discrete batches of magmas.

The critical issue is that the less-evolved magma pulses, whatever the origin of their Sr isotope signature, evolve along liquid lines of descent from shoshonite through latite and trachyte without any increase in $^{87}Sr/^{86}Sr$ (Fig. 7), and $^{143}Nd/^{144}Nd$ (Fig. 6c). The broadly horizontal liquid lines of descent displayed by the samples (Fig. 7) are thus consistent with a closed system fractional crystallization process, and all Ischia volcanic rocks evolve along similar liquid lines of descent (Figs. 3, 4) independent on differences in radiogenic isotope composition. Moreover, it is noteworthy to highlight the significant spread of Sr isotope composition at similar degree of differentiation, also within a single eruptive phase (Fig. 8). This is obviously true for the highly-evolved trachytes with $^{87}Sr/^{86}Sr_i > 0.707$, but also for other samples, especially within V Phase. Considering a vertically stratified magma chamber, this evidence implies that magmas with similar major and trace element composition, thus hypothetically at the same level, have not been fully re-homogenized. Hence, Sr isotopes are consistent with a more complex structure of the reservoir made up by isolated pockets of melts with broadly similar crystallization history that did not actually interact with each other (e.g., Cashman & Giordano, 2014).

The highly-evolved trachytes with $^{87}Sr/^{86}Sr_i>0.707$ do not make an exception to this rule, and are indistinguishable from other samples at the same degree of evolution considering all major and trace elements (Figs. 3, 4), and radiogenic isotopes but $^{87}Sr/^{86}Sr$ (Figs. 7, 8). However, their anomalous Sr isotope compositions, coupled with their high Rb/Sr can provide constraints on the magma storage timescales of Ischia volcano. The following discussion will be focused on these samples that have never been given a detailed assessment despite they can reveal important implications on the magma chamber dynamics at Ischia.

Always consult and cite the final, published document. See http:/www.minsocam.org or GeoscienceWorld

The origin of trachytes with $^{87}Sr/^{86}Sr_i$ >0.707

The anomalous highly-evolved trachytes with $^{87}Sr/^{86}Sr_i$>0.707 do not comply with the proposed closed system differentiation trend, since there is no less-evolved counterpart (i.e., shoshonite) with similar $^{87}Sr/^{86}Sr_i$ at high Sr (and also CaO) content (Figs. 7, 8). The first, and perhaps more obvious, explanation that could account for their anomalous Sr isotope composition is the occurrence of open system processes with assimilation of country rocks. To constrain the potential role of crustal assimilation, we modelled an Energy Constrained Assimilation and Fractional Crystallization (EC-AFC) process (Spera & Bohrson, 2001) operating on trachytic magma during the second step of fractional crystallization (Brown et al., 2014). The results are reported in Table 2, plotted in Fig. 7, and in Supplementary Table S3. As assimilated material, we used both the average composition of the Hercynian Calabrian basement (Fornelli et al., 2002) and the GLOSS (Plank & Langmuir, 1998) as a reference. The modelled EC-AFC process, albeit apt to increase the Sr isotope composition of evolving magmas, is unable to reproduce the low Sr content measured in the highly-evolved trachytes (from 34 to 4 ppm, Fig. 7). At the temperature of these highly-evolved trachytes (some 750°C, Fig. 4) the modelled liquid lines of descent of both assimilation scenarios yield Sr content >140 ppm and $^{87}Sr/^{86}Sr$ > 0.714 (Fig. 7), which are not compatible with the observed compositions. This is because the relatively high Sr content of the assimilated crustal material (both Hercynian Calabrian basement and GLOSS, Table 2) yields a liquid line of descent towards increasing $^{87}Sr/^{86}Sr$ with a Sr content threshold (some 25 ppm at ~810°C, Fig. 7**)** significantly higher than the observed values in the highly-evolved trachyte samples. Moreover, crustal contamination is expected to produce a coherent Nd isotope composition variation from shoshonite to latite and trachyte (Table S3), whilst the highly-evolved trachytes have $^{143}Nd/^{144}Nd$ identical to the other more- and less-evolved magmas of the corresponding activity phase (Fig. 6c).

Always consult and cite the final, published document. See http:/www.minsocam.org or GeoscienceWorld

In order to investigate the magmatic processes forming the anomalously high radiogenic Sr trachytes, we compared the major and trace element composition of these samples with the overall trend described by Ischia magmas. As stated above, the high radiogenic Sr trachytes fall along a common liquid line of descent with other samples, showing no significant differences from "normal" trachytes (Figs. 3, 4). The same is true for Nd isotopes which are within the range of other samples with "normal" $^{87}Sr/^{86}Sr_i$ (Fig. 6c). This means that the origin of their high radiogenic Sr isotope composition must be related to magmatic processes that did not significantly affect the major, trace element, and Nd isotope composition of the magmas, but only their Sr isotope composition, such as time-related radiogenic ^{87}Sr in-growth.

The trachyte samples with $^{87}Sr/^{86}Sr_i$ >0.707 are characterized by elevated $^{87}Rb/^{86}Sr$ (up to 667, Fig. 9), developed during the second step of crystal fractionation. These high Rb-Sr ratios imply that isolated trachytic magma portions, remaining in a partially liquid state even for only a few tens of thousands of years, are liable to develop significant ^{87}Sr in-growth and become more radiogenic than other portions of the magma chamber (e.g., Davies and Halliday, 1998; Heumann, 1999; Heumann and Davies, 2002; Heumann et al., 2002; Simon & Reid, 2005; Crowley et al., 2007; Chamberlain et al., 2014)

On the basis of the correlation between $^{87}Sr/^{86}Sr_i$ and $^{143}Nd/^{144}Nd$ (Fig. 5), we assumed that the anomalously high radiogenic Sr trachytes had a nominal $^{87}Sr/^{86}Sr$ of ca. 0.7065 at the time of their formation in the Ischia volcanic system. This Sr isotope composition would suggest a hypothetical magma residence time between 210 kyr and 1.9 Myr (Fig.9). These timescales, however, have to be considered as indicative, due to the significant uncertainty in the measured Rb/Sr because of the low Sr content of the samples (a few ppm determined by ICP-MS, Supplementary Table S2), and to the somewhat arbitrary choice of starting Sr isotope composition.

To further explore this hypothesis and place more robust constraints on magma residence time in the active volcanic system at Ischia, we carried out high-quality Rb-Sr isotope dilution and Sr

Always consult and cite the final, published document. See http:/www.minsocam.org or GeoscienceWorld

isotope composition analyses on separated mineral fraction and either groundmass or glass (hereafter generally indicated as groundmass) pairs. We selected a number of phenocryst-groundmass pairs in trachyte samples with both *anomalous* $^{87}Sr/^{86}Sr$ (ISC 10-01 and ISC 10-05) and, by comparison, *normal* $^{87}Sr/^{86}Sr$ (ISC 10-04 and ISC 10-08, i.e., in the same range of the other volcanic products, Fig. 9). The rationale is that the radiogenic ^{87}Sr in-growth process, if any, must have left a record in the Sr isotope composition of phenocrysts occurring in the trachyte magmas.

Residence time analysis

The Rb-Sr isotope dilution, and $^{87}Sr/^{86}Sr$ isotope composition analyses performed on groundmass and mineral separates are reported in Table 3, along with mineral residence times obtained by subtracting the known K-Ar eruption age (Gillot et al., 1982; Poli et al., 1987; Tibaldi and Vezzoli, 2004) from the mineral-groundmass Rb-Sr age. The results are also plotted in Fig. 10, using a backward modelling approach to calculate the time t_0 at which each phenocryst-groundmass pair had the same $^{87}Sr/^{86}Sr$ starting from the measured $^{87}Sr/^{86}Sr$ and $^{87}Rb/^{86}Sr$.

All of the samples yield variable timescale information predating the eruption age from some 4 kyr to 890 kyr (Table 3), indicating that the long-lived storage timescale is not restricted to the *anomalous* $^{87}Sr/^{86}Sr$ trachytes but also to the *normal* $^{87}Sr/^{86}Sr$ trachytes (Fig. 10). The two samples with *normal* $^{87}Sr/^{86}Sr$ (ISC 10-04, ISC 10-08), along with one of the samples with *anomalous* $^{87}Sr/^{86}Sr$ (ISC 10-05) yield similar timescale information (from 4.2 kyr to 34 kyr, Fig. 10b, c, d). The other *anomalous* $^{87}Sr/^{86}Sr$ trachyte sample (ISC 10-01) yields timescale information from 640 kyr (clinopyroxene) to 890 kyr (sanidine) (Fig. 10a). Based on the assumption of chemical equilibrium during crystallization and subsequent negligible Sr isotope homogenization via diffusion, the timescale information obtained from phenocryst-groundmass pairs (Table 3) could be interpreted as magma residence times. Chemical equilibrium between sanidine-groundmass pairs has been ascertained by careful petrographic analyses of thin sections demonstrating no evidence of

Always consult and cite the final, published document. See http:/www.minsocam.org or GeoscienceWorld

reaction textures, as also confirmed by a previous study (Melluso et al., 2014). Sr diffusion coefficient in minerals is strongly dependent upon temperature, and the degree of Sr isotope homogenization can be modelled applying the Equation 6.20 from Crank (1975) for diffusion in a sphere. The estimated temperature of samples at the same degree of evolution as the analysed trachytes (Fig. 4) is 700-770°C (Melluso et al., 2014). Sr chemical diffusion in sanidine at a nominal temperature of 750°C is $9.0 \cdot 10^{-19}$ cm^2s^{-1} (Cherniak, 1996), implying that Sr isotope homogenization in a crystal with a radius of 2 mm is <2% after 27 kyr (e.g., ISC 10-05, Table 3), and still < 8 % even after 890 kyr (ISC 10-01, Table 3). Another constraint on the occurrence of negligible Sr isotope homogenization is provided by the overall Sr isotope dataset. The range of the calculated Sr isotope composition of sanidine-groundmass pairs at the time of crystallization t_0 is between 0.7062-0.7067 (Table 3, Fig. 10). If significant Sr isotope homogenization had occurred (i.e., using wrong temperature estimates), this would result in sanidine with $^{87}Sr/^{86}Sr$ <0.7062 at the time of crystallization, contrary to the Sr isotope signature exhibited by the feeding magmas at low Rb/Sr (Fig. 9). This means that the calculated residence times, albeit only on 4 samples, can be considered reliable estimates.

Sr diffusion in clinopyroxene is orders of magnitudes lower than in sanidine at 750°C (Sneeringer et al., 1984), and the single clinopyroxene-groundmass pair measured for sample ISC10-01 yields a calculated residence time of 640 kyr, significantly shorter than that calculated for sanidine in the same sample (Fig. 10a). The different residence times can correspond to the actual crystallizing succession during the second step. Indeed, differentiation modelling performed with Rhyolite-MELTS (Gualda et al., 2012) suggests that, in the absence of plagioclase, sanidine precedes clinopyroxene in the crystallization sequence. An alternative hypothesis could be that the clinopyroxene derives from mingling processes with a successive pulse of highly-evolved trachytic magma, although we do not have arguments to assess which hypothesis is more reliable.

Always consult and cite the final, published document. See http:/www.minsocam.org or GeoscienceWorld

The long-lived storage time of sample ISC10-01 (Fig. 10a) is somewhat puzzling, although the oldest age of volcanic rocks at Ischia (150 ka) is limited to the subaerial portion and not to the entire volcanic edifice below sea level. Admittedly, more data are needed to confirm the timescale obtained by this single sample, and have a comprehensive scenario on the onset of volcanic activity at Ischia, although in the Pontine Islands, just a few km north of Ischia, K-rich magmatism is dated back at 1 Ma (Cadoux et al., 2005).

In summary, our results indicate that a number of more-evolved trachytic magmas remained stored for variable timescales (Fig. 10) in isolated pockets within the magma chamber at relatively low temperature (~750°C), in agreement with the estimates of Melluso et al. (2014). It is noteworthy that also the samples with *normal* $^{87}Sr/^{86}Sr$ (Fig. 9) yield a magma residence time before eruption from 4 to 27 kyr (Table 3, Fig. 10c, d), implying that the low-T storage is not limited to the *anomalous* $^{87}Sr/^{86}Sr$ trachytes (Fig. 9), but could be a characteristic of the magma chamber dynamics of the active Ischia volcano. The assessment of pre-eruptive time information in less-evolved magmatic products of Ischia remains, however, undisclosed for two reasons: (i) the high temperature of these magmas (1030-930°C, Fig. 4), enhancing Sr isotope homogenization and resetting any time-related information, and (ii) their relatively low Rb/Sr (Fig. 9), preventing to achieve phenocryst-groundmass Sr isotope differences beyond current external reproducibility of Sr isotope measurements via TIMS ($2\sigma = 1\text{-}1.5\ 10^{-5}$, e.g., Avanzinelli et al., 2005) in only a few tens of thousands of years.

Implications for magma chamber dynamics

The magma chamber dynamics of the active Ischia volcano consists of alternating periods of magma recharge, differentiation, eruption, and quiescence from at least 150 kyr to present (e.g., Poli et al., 1989; Civetta et al., 1991; de Vita et al., 2010; D'Antonio et al., 2013; Brown et al., 2014). The erupted magmas record an evolutionary process consisting of recurrent two-step fractional

Always consult and cite the final, published document. See http:/www.minsocam.org or GeoscienceWorld

crystallization events (Brown et al., 2014), controlling extreme trace element variations such as low Sr and high Rb contents along with high La/Sm in more-evolved trachytes. Remarkably, no distinction is observed in the differentiation pathways of each magma pulse with distinct Sr isotope composition. The lack of systematic Sr and Nd isotope co-variation during magmatic differentiation from shoshonite to latite, and trachyte indicates that the overall isotopic variability cannot be related to a simple process of contamination by crustal material. The Sr, and to a minor extent Nd, isotope variability at similar degree of differentiation, even within a given activity phase, suggests that the magmas erupted at Ischia do not come from a single re-homogenized reservoir. And this is consistent with multiple magma pockets that have remained isolated within the volcano feeding system, despite following similar differentiation pathways, according to the model of Cashman & Giordano (2014).

The occurrence of a number of highly-evolved trachytes with extremely low Sr contents and high Rb/Sr, having anomalously high radiogenic $^{87}Sr/^{86}Sr$, reinforces this interpretation and sets constraints on magma storage timescale at Ischia. The high radiogenic Sr isotope signature cannot be ascribed to crustal contamination processes, and implies a long-lived history of magma storage, in the order of a few tens to hundreds of thousands of years. Rb-Sr isochrons on separated mineral-groundmass pairs set compelling evidence on the occurrence of variable magma residence timescales in the active Ischia volcanic system. Such variable residence times are consistent with storage of the most differentiated magmas at relatively low temperature (~750°C), within isolated magma chamber pockets (e.g., Cashman & Giordano, 2014; Cooper & Kent, 2014). These more-evolved magma pockets have to be stored in a partially liquid-state in order to develop radiogenic ^{87}Sr in-growth. Consequently, given the relatively shallow-depth of the Ischia magma chamber (~6-7 km, Piochi, 1995; Moretti et al., 2013; Brown et al., 2014, and reference therein), these pockets must necessarily be in a steady-state thermal flux regime to maintain the estimated temperature of ~750°C, and there must be no mass exchange with other, less-evolved, portions of the magma

Always consult and cite the final, published document. See http:/www.minsocam.org or GeoscienceWorld

chamber to preserve low Sr content and high Rb/Sr (i.e., overall magma chamber recharge without chemical interaction). The occurrence of high average heat flow of some 500 mWm^2 (Carlino et al., 2014) support the possibility to maintain storage of magma pockets in a partially liquid-state.

The magma chamber dynamics of the active Ischia volcano, probed on the basis of geochemical and radiogenic isotope signatures, is consistent with recent models of complex magma chamber reservoirs made up of multiple melt lenses isolated by largely crystalline mush portions (Cashman and Giordano, 2014), and opens new scenarios to future studies on this active volcano.

Acknowledgements

We greatly acknowledge Lorella Francalanci for focusing and stirring the discussion on early drafts of the manuscript. We are also grateful to Maurizio Ulivi for his skilful assistance and technical support during isotope analyses and laboratory management, and Giovanni Orsi for his precious hints during field work planning. The criticism of Katy Chamberlain and Massimo D'Antonio greatly improved the manuscript**.** Financial support has been provided by MIUR grants 2004040502_001, 2008HMHYFP_002, and 2010TT22SC_001 to S.C., R.A., and S.T.

References Cited

Acocella, V., and Funiciello, R. (1999) The interaction between regional and local tectonic during resurgent doming: the case of the island of Ischia, Italy. Journal of Volcanology and Geothermal Research, 88, 109-123.

Acocella, V., Cifelli, F., Funiciello, R. (2001) The control of overburden thickness on resurgent domes: insights from analogue models. Journal of Volcanology and Geothermal Research, 111, 137-153.

Acocella, V., Marotta, E., Funiciello, R., Orsi, G., de Vita, S. (2004) The role of extensional structures on experimental calderas and resurgence. Journal of Volcanology and Geothermal Research, 129, 199-217.

Always consult and cite the final, published document. See http:/www.minsocam.org or GeoscienceWorld

Ajuso, R.A., De Vivo, B., Rolandi, G., Seal, R.R., Paone, A. (1998) Geochemical and isotopic (Nd-Pb-Sr-O) variations bearing on the genesis of volcanic rocks from Vesuvius, Italy. Journal of Volcanology and Geothermal Research, 82, 53-78.

Alloway, B.V., Pearce, N.J.G., Villarosa, G., Outes, V., Moreno, P.I. (2015) Multiple melt bodies fed the AD 2011 eruption of Puyehue-Cordón Caulle, Chile. Scientific Reports, 5, 17589.

Andria, M.C. (2008) Studio dell'evoluzione del sistema magmatico dell'Isola d'Ischia, Italia Meridionale, negli ultimi 10 ka. Ph.D. thesis, Università degli studi di Trieste (in Italian), 140 p.

Appleton, J.D. (1972) Petrogenesis of Potassium-rich Lavas from the Roccamonfina Volcano, Roman Region, Italy. Journal of Petrolology, 13, 425-456.

Avanzinelli, R., Boari, E., Conticelli, S., Francalanci, L., Guarnieri, L., Perini, G., Petrone, C.M., Ulivi, M., Tommasini, S. (2005) High precision Sr, Nd and Pb isotopic analyses using the new generation Thermal Ionization Mass Spectrometer ThermoFinnigan Triton-Ti. Periodico di Mineralogia, 75, 3, 147-166.

Avanzinelli, R., Elliot, T., Tommasini, S., Conticelli, S. (2008) Constraints on the Genesis of Potassium-rich Italian Volcanic Rocks from U/Th Disequilibrium. Jurnal of Petrology, 49, 2, 195-223.

Avanzinelli, R., Lustrino, M., Mattei, M., Melluso, L., Conticelli, S. (2009) Potassic and ultrapotassic magmatism in the circum-Tyrrhenian region: significance of carbonated pelitic vs. pelitic sediment recycling at destructive plate margin. Lithos, 133, 213-227.

Bachmann, O., and Bergantz, G.W. (2004) On the origin of crystal-poor rhyolites: Extracted from batholithic crystal mushes. Journal of Petrology, 45, 1565-1582.

Bachmann, O., and Bergantz, G.W. (2008b) Rhyolites and their source mushes across tectonic settings. Journal of Petrology, 49, 2277-2285.

Bachmann, O., and Bergantz, G.W. (2008a) Deciphering magma chamber dynamics from styles of compositional zoning in large silicic ash flow sheets. Reviews in Mineralogy and Geochemistry, 69, 651-674.

Baldridge, W., Carmichael, I.S.E., Albee, A.L. (1981) Crystallization paths of leucite-bearing lavas: examples from Italy. Contribution to Mineralogy and Petrology, 76, 3, 321-35.

Barker, A.K., Troll, V.R., Carracedo, J.C., Nicholls, P.A. (2015) The magma plumbing system for the 1971 Teneguía eruption on La Palma, Canary Islands. Contributions to Mineralogy and Petrology, 170, 54.

Beccaluva L., Di Girolamo, P., Serri, G. (1991) Petrogenesis and tectonic setting of the Roman Volcanic Province, Italy. Lithos, 26, 191-221.

Always consult and cite the final, published document. See http:/www.minsocam.org or GeoscienceWorld

Braschi, E., Francalanci, L., Vougioukalakis, G.E. (2012) Inverse differentiation pathway by multiple mafic magma refilling in the last magmatic activity of Nisyros Volcano, Greece. Bullettin of Volcanology, 74, 1083-1100.

Brown, R.J., Orsi, G., de Vita, S. (2008) New insights into Late Pleistocene explosive volcanic activity and caldera formation on Ischia (southern Italy). Bulletin of Volcanology, 70, 583-603.

Brown, R.J., Civetta, L., Arienzo, I., D'Antonio, M., Moretti, R., Orsi, G., Tomlinson, E.L., Albert, P.G., Menzies, M.A. (2014) Geochemical and isotopic insights into the assembly, evolution and disruption of a magmatic plumbing system before and after a cataclysmic caldera collapse eruption at Ischia volcano (Italy). Contribution to Mineralogy and Petrology, 168, 3, 1-23.

Buchner, G., Italiano, A., Vita-Finzi, C. (1996) Recent uplift of Ischia southern Italy. Geological Society of London, Special Publications, 110, 1, 249-252.

Cadoux, A., Pinti, D.L., Aznar, C., Chiesa, S., Gillot, P.Y. (2005) New chronological and geochemical constraints on the genesis and geological evolution of Ponza and Palmarola Volcanic Islands (Tyrrhenian Sea, Italy). Lithos, 81, 121-151.

Caprarelli, G., Togashi, S., De Vivo, B. (1993) Preliminary Sr and Nd isotopic data for recent lavas from Vesuvius volcano. Journal of Volcanology and Geothermal Research, 58, 1, 377-381.

Carlino, S., Somma, R., Troiano, A., Di Giuseppe, M.G., Troise, C., De Natale, G. (2014) The geothermal system of Ischia Island (southern Italy): Critical review and sustainability analysis of geothermal resource for electricity generation. Renewable Energy, 62, 177-196.

Cashman, K.V., and Giordano, G. (2014) Calderas and magma reservois. Journal of Volcanology and Geothermal Research, 288, 28-45.

Chamberlain, K.J., Morgan, D.J., Wilson, C.J.N. (2014) Timescales of mixing and mobilisation in the Bishop Tuff magma body: perspectives from diffusion chronometry. Contributions to Mineralogy and Petrology, 168, 1034.

Cherniak, D.J. (1996) Strontium diffusion in sanidine and albite, and general comments on strontium diffusion in alkali feldspars. Geochimica and Cosmochimica Acta, 60, 5037-5043.

Chiodini, G., Avino, R., Brombach, T., Caliro, S., Cardellini, C., De Vita, S., Frondini, F., Granirei, D., Marotta, E., Ventura, G. (2004) Fumarolic and diffuse soil degassing west of Mount Epomeo, Ischia, Italy. Journal of Volcanology and Geothermal Research, 133, 291-309.

Civetta, L., Gallo, G., Orsi, G. (1991) Sr- and Nd- isotope and trace-element constraints on the chemical evolution of the magmatic system of Ischia (Italy) in the last 55 ka. Journal of Volcanology and Geothermal Research, 46, 213-230.

Always consult and cite the final, published document. See http:/www.minsocam.org or GeoscienceWorld

Cooper, K.M., and Kent, A.J. (2014) Rapid remobilization of magmatic crystals kept in cold storage. Nature, 506(7489), 480-483.

Conticelli, S., and Peccerillo, A. (1992) Petrology and geochemistry of potassic and ultrapotassic volcanism in Central Italy: petrogenesis and interferences on the mantle source. Lithos, 28, 221-240.

Conticelli, S., D'Antonio, M., Pinarelli, L., Civetta, L. (2002) Source contamination and mantle heterogeneity in the genesis of Italian potassic and ultrapotassic volcanic rocks: Sr-Nd-Pb isotope data from Roman Province and Southern Tuscany. Mineralogy and Petrology, 74, 189-222.

Conticelli, S., Melluso, L., Perini, G., Avanzinelli, R., Boari, E. (2004) Petrologic, geochemical and isotopic characteristics of potassic and ultrapotassic magmatism in Central-Southern Italy: inferences on its genesis and on the nature of mantle sources. Periodico di Mineralogia, 73, 135-164.

Conticelli, S., Marchionni, S., Rosa, D., Giordano, G., Boari, E., Avanzinelli, R. (2009) Shoshonite and sub-alkaline magmas from an ultrapotassic volcano: Sr-Nd-Pb isotope data on the Roccamonfina volcanic rocks, Roman Magmatic Province, Southern Italy. Contributions to Mineralogy and Petrology, 157, 41-63.

Conticelli, S., Laurenzi, M.A., Giordano, G., Mattei, M., Avanzinelli, R., Melluso, L., Tommasini, S., Boari, E., Cifelli, F., Perini, G. (2010) Leucite-bearing (kamafugitic/leucititic) and -free (lamproitic) ultrapotassic rocks and associated shoshonites from Italy: constraints on petrogenesis and geodynamics. In: Beltrando, M., Peccerillo, A., Mattei, M., Conticelli, S., Doglioni, C., Eds. The Geology of Italy. Journal of Virtual Explorer, 36, p.20.

Conticelli, S., Boari, E., Burlamacchi, L., Cifelli, F., Moscardi, F., Laurenzi, M.A., Ferrari Pedraglio, L., Francalanci, L., Benvenuti, M.G., Braschi, E., Manetti, P. (2015a) Geochemistry and Sr-Nd-Pb isotopes of Monte Amiata volcano, Central Italy: evidence for magma mixing between high-K calc-alkaline and leucititic mantle-derived magmas. Italian Journal of Geosciences, 134, 266-290.

Conticelli, S., Avanzinelli, R., Ammannati, E., Casalini, M. (2015b) The role of carbon from recycled sediments in the origin of ultrapotassic igneous rocs in the Central Mediterranean. Lithos, 232, 174-196.

Crank, J. (1975) The mathematics of diffusion, 414 p. Oxford University Press, London.

Crisci, G.M., De Francesco, A.M., Mazzuoli, R., Poli, G., Stanzione, D. (1989) Geochemistry of the recent volcanics of Ischia Island, Italy: Evidence of crystallization and magma mixing. Chemical Geology, 78, 15-33.

Always consult and cite the final, published document. See http:/www.minsocam.org or GeoscienceWorld

Crowley, J.L., Schoene, B., Bowring, S.A. (2007) U-Pb dating of zircon in the Bishop Tuff at the millennial scale. Geology, 35, 12, 1123-1126.

Cubellis, E., Carlino, S., Iannuzzi, R., Luongo, G., Obrizzo, F. (2004) Management of hystorical seismic data using GID: the Island of Ischia (Southern Italy). Natural Hazard, 33, 379-393.

D'Antonio, M., Civetta, L., Di Girolamo, P. (1999) Mantle source heterogeneity in the Campanian Region (South Italy) as inferred from geochemical and isotopic features of mafic volcanic rocks with shoshonitic affinity. Mineralogy and Petrology, 67, 163-192.

D'Antonio, M., Tonarini, S., Arienzo, I., Civetta, L., Di Renzo, V. (2007) Components and processes in the magma genesys of the Phleagran Volcanic District, southern Italy. In: Beccaluva, L., Bianchini, G., Wilson, M. Eds. Cenozoic volcanism in the Mediterranean Area, 418, p. 203-220. Geological Society of America Special Papers.

D'Antonio, M., Tonarini, S., Arienzo, I., Civetta, L., Dallai, L., Moretti, R., Orsi, G., Andria, M., Trecalli, A. (2013) Mantle and crustal processes in the magmatism of the Campanian region: inferences from mineralogy, geochemistry, and Sr-Nd-O isotopes of young hybrid volcanics of the Ischia island (South Italy). Contribution to Mineralogy and Petrology, 165, 1173-1194.

Davies, G.R., and Halliday, A.N. (1998) Development of the Long Valley rhyolitic magma system: Strontium and neodymium isotope evidence from glasses and individual phenocrysts. Geochimica and Cosmochimica Acta, 62, 21/22, 3561-3574.

Della Seta, M., Marotta, E., Orsi, G., de Vita, S., Sansivero, F., Fredi, P. (2012) Slope instability induced by volcano-tectonics as an additional source of hazard in active volcanic areas: the case of Ischia island (Italy). Bullettin of Volcanology, 74, 79-106.

de Vita, S., Sansivero, F., Orsi, G., Marotta, E. (2006) Cyclical slope instability and volcanism related to volcano-tectonism in resurgent calderas: The Ischia Island (Italy) case study. Engineering Geology, 86, 148-165.

de Vita, S., Sansivero, F., Orsi, G., Marotta, E., Piochi, M. (2010) Volcanological and structural evolution of the Ischia resurgent caldera (Italy) over te past 10 ka. In: Groppelli, G., Viereck-Goette, L., Eds, Stratigraphy and geology of volcanic areas, 464, p.193-239. Geological Society of America Special Papers.

Di Girolamo, P., Melluso, L., Morra, V., Secchi, F.A.G. (1995) Evidence of interaction between mafic and differentiated magmas in the youngest phase of activity at Ischia Island (Italy). Periodico di Mineralogia, 64, 393-411.

Di Napoli, R., Martorana, R., Orsi, G., Aiuppa, A., Camarda, M., De Gregorio, S., Gagliano Candela, E., Luzio, D., Messina, N., Pecoraino, G., Bitetto, M., de Vita, S., Valenza, M.

Always consult and cite the final, published document. See http:/www.minsocam.org or GeoscienceWorld

(2011) The structure of a hydrothermal system from an integrated geochemical, geophysical and geological approach: the Ischia Island case study. Geochemistry Geophysics Geosystems, 12, 7, Q07017.

Elliott, T. (2003) Tracers of the slab. In Eiler, J.M., Ed., Inside the Subduction factory, p. 23-45. American Geophysical Union.

Ellis, B.S., Bachmann, O., Wolff, J.A. (2014) Cumulate fragments in silicic ignimbrites: The case of the Snake River Plain. Geology 42, 431-434.

Fedele, L., Zanetti, A., Morra, V., Lustrino, M., Melluso, L., Vannucci, R. (2009) Clinopyroxene/liquid trace element partitioning in natural trachyte–trachyphonolite systems: insights from Campi Flegrei (southern Italy). Contributions to Mineralogy and Petrology, 158, 337-356.

Fedele, L., Lustrino, M., Melluso, L., Morra, V., Zanetti, A., Vannucci, R. (2015) Trace-element partitioning between plagioclase, alkali feldspar, Ti-magnetite, biotite, apatite, and evolved potassic liquids from Campi Flegrei (Southern Italy). American Mineralogist, 100, 233-249.

Fornelli, A., Piccarreta, G., Del Moro, A., Acquafredda, P. (2002) Multi-stage Melting in the Lower Crust of the Serre (Southern Italy). Journal of Petrology 43, 12, 2191-2217.

Francalanci, L., Davies, G.R., Lustenhouwer, W., Tommasini, S., Mason, P.R.D., Conticelli, S. (2005) Intra-grain Sr isotope evidence for crystal recycling and multiple magma reservoirs in the recent activity of Stromboli volcano, southern Italy. Journal of Petrology, 46, 1997-2021.

Gasperini, D., Blichert-Toft, J., Bosch, D., Del Moro, A., Macera, P., Albarede, F. (2002) Upwelling of deep mantle material through a plate window: evidence from the geochemistry of Italian basaltic volcanics. Journal of Geophysical Research, 107, 7-19.

Gillot, P.Y., Chiesa, S., Pasquarè, G., Vezzoli, L. (1982) 33.000 yr K/Ar dating of the volcano-tectonics horst of the island of Ischia, Gulf of Naples. Nature, 229, 242-245.

Gualda, G.A.R., Ghiorso, M.S., Lemons, R.V., Carley, T.L. (2012) Rhyolite-MELTS: A modified calibration of MELTS optimized for silica-rich, fluid-bearing magmatic systems. Journal of Petrology, 53, 875-890.

Gudmundsson, A. (2012) Magma chambers: Formation, local stresses, excess pressures, and compartments. Journal of Volcanology and Geothermal Research, 237-238, 19-41.

Halliday, A.N., Davidson, J.P., Hildreth, W., Holden, P. (1991) Modelling the petrogenesis of high Rb/Sr silicic magmas. Chemical Geology, 92, 107-114.

Heumann, A. (1999) Timescales of processes within silicic magma chambers. PhD Thesis, Department of Petrology and Isotope Geology, University of Amstardam, p. 196.

Always consult and cite the final, published document. See http:/www.minsocam.org or GeoscienceWorld

Heumann, A., and Davies, G.R. (2002) U-Th disequilibrium and Rb-Sr age constraints on the magmatic evolution of peralkaline rhyolites from Kenia. Journal of Petrology, 43, 3, 557-577.

Heumann, A., and Davies, G.R., Elliott, T. (2002) Crystallization history of rhyolites at Long Valley, California, inferred from combined U-series and Rb-Sr isotope systematics. Geochimica et Cosmochimica Acta, 66, 10, 1821-1837.

Hildreth, W. (2004) Volcanological perspectives on Long Valley, Mammoth Mountain, and Mono Craters: Several contiguous but discrete systems. Journal of Volcanology and Geothermal Research, 136, 169-198.

Huppert, H.E., and Woods, A.W. (2002) The role of volatiles in magma chamber dynamics. Nature, 420, 493-495.

Inguaggiato, S., Pecoraino, G., D'Amore, F. (2000) Chemical and isotopical characterisation of fluid manifestations of Ischia Island (Italy). Journal of Volcanology and Geothermal Research, 99, 99-178.

Joron, J.L., Metrich, N., Rosi, M., Santacroce, R., Sbrana, A. (1987) Chemistry and petrography. Somma-Vesuvius, CNR Quaderni Ricerca Scientifica 114, 105-174.

Le Maitre, R.W., Bateman, P., Dudek, A., Keller, J., Lameyr, J., Le Bas, M.J., Sabine, P.J., Schmid, R., Sørensen, H., Streckeisen, A., Wooley, A.R., Zanettin, B., (eds) (1989) A classification of igneous rocks and glossary terms: recommendations of the International Union of Geological Sciences, Subcommission on the Systematics of Igneous Rocks, 193 p. Blackwell Scientific, Oxford.

Marotta, E., and de Vita, S. (2014) The role of pre-existing tectonic structures and magma chamber shape on the geometry of resurgent blocks: analogue models. Journal of Volcanology and Geothermal Research, 272, 23-38.

Marsh, B.D. (2006) Dynamics of magmatic systems. Elements 2, 287-292.

Mazzeo, F.C., D'Antonio, M., Arienzo, I., Aulinas, M., Di Rienzo, V., Gimeno, D., (2014) Subduction-related enrichment of the Neapolitan Volcanoes (Southern Italy) mantle source: New constraints on the characteristics of the slab-derived components. Chemical Geology 386, 165-183.

Melluso, L., de' Gennaro, R., Fedele, L., Franciosi, L., Morra, V. (2012) Evidence of crystallization in residual, Cl-F-rich agpaitic, trachyphonolitic magmas and primitive Mg-rich basalt-trachyphonolite interaction, in the lava domes of the Phleagran Fields (Italy). Geological Magazine, 149, 532-550.

Always consult and cite the final, published document. See http:/www.minsocam.org or GeoscienceWorld

Melluso, L., Morra, V., Guarino, R., de' Gennaro, R., Franciosi, L., Grifa, C. (2014) The crystallization of shoshonitic to pralkaline trachyphonolitic magmas in a H2O-Cl-F-rich environment at Ischia (Italy), with implications for the feeder system of the Campania Plain volcanoes. Lithos, 210, 242-259.

Monti, L., Sbrana, A., Toccaceli, R.M., Faccenna, C., Fulignati, P., Giudetti, G., Marianelli, P., Deino, A., Bravi, S., D'Argenio, B., Marsella, E., Putignano, M.L., de Alteriis, G., De Lauro, M., Di Martino, G., D'Isanto, C., Giordano, F., Innangi, S., Passaro, S., Scotto di Vettimo, P., Tonielli, R., Aiello, G., Budillon, F., Conforti, A., Ferraro, L., Capodanno, M., Molisso, F., Luperini, W., Marianelli, P., Vietina, M., Donadio, C., Priore, A., Terlizzi F. (2010) Carta Geologica d'Italia alla scala 1:25.000 – Foglio 464 Isola d'Ischia, Progetto Car.G, Regione Campania, ISPRA, SystemCart, Roma; http://www.isprambiente.gov.it/MEDIA/carg/464_ISOLA_DISCHIA/Foglio.html

Moretti, R., Arienzo, I., Orsi, G., Civetta, L., D'Antonio, M. (2013) The deep plumbing system of Ischia: a physico-chemical window on the fluidsaturated and CO2-sustained Neapolitan volcanism (southern Italy). Journal of Petrology, 54, 951-984.

Orsi, G., Gallo, G., Zanchi, A. (1991) Simple-shearing block resurgence in caldera depressions. A model from Pantelleria and Ischia. Journal of Volcanology and Geothermal Research, 47, 1-11.

Orsi, G., Gallo, G., Heikien, G., Wohletz, K., Yu, E., Bonani, G. (1992) A comprehensive study of pumice formation and dispersal: the Cretaio Tephra of Ischia (Italy). Journal of Volcanology and Geothermal Research, 53, 1, 329-354.

Orsi, G., Piochi, M., Campajola, L., D'Onofrio, A., Gialanella, L., Terrasi, F. (1996) 14C geochronological constraints for the volcanic history of the island of Ischia (Italy) over the last 5000 years. Journal of Volcanology and Geothermal Research, 71, 249-257.

Orsi, G., de Vita, S., Di Vito, M., Isais, R., Nave, R., Heiken, G. (2003) Facing volcanic and related hazards in the Neapolitan area. In: Heiken, G., Fakundiny, R., Sutter, J., Eds, Earth Sciences in Citiesp. 121-170, American Geophysical Union (Special Publication), Washington.

Peccerillo, A. (1999) Multiple mantle metasomatism in Central-Southern Italy: Geochemical effects, timing and geodynamic implications. Geology, 27, 315-318.

Peccerillo, A. (2001) Geochemical similarities between the Vesuvius, Phlaegrean Fields and Stromboli volcanoes: petrogenetic, geodynamic and volcanological implications. Mineralogy and Petrology, 73, 93-105.

Peccerillo, A. (2005) Plio-Quaternary Volcanism in Italy, 365 p. Springer-Verlag Berlin Heidelberg.

Always consult and cite the final, published document. See http:/www.minsocam.org or GeoscienceWorld

Peccerillo, A., and Manetti, P. (1985) The potassium alkaline volcanism of central-southern Italy; a review of the data relevant to petrogenesys and geodynamic significance. South African Journal of Geology, 88, 2, 379-394.

Piochi, M. (1995) The Ischia magmatic system in the last 10 ka: geochemical and geophysical evidence. Plinius, 13, 190-19.

Piochi, M., Civetta, L., Orsi, G. (1999) Mingling in the magmatic system of Ischia in the past 5 ka. Mineralogy and Petrology, 66, 227-258.

Plank,T., and Langmuir, C. H. (1998) The chemical composition of subducting sediment and its consequences for the crust and mantle. Chemical Geology, 145, 325-394.

Poli, S., Chiesa, S., Gillot, P.Y., Gregnain, A., Guichard, F. (1987) Chemistry versus time in the volcanic complex of Ischia (Gulf of Naples, Italy) evidence of successive magmatic cycles. Contribution to Mineralogy and Petrology, 95, 322-235.

Poli, S., Chiesa, S., Gillot, P.Y., Guichard, F., Vezzoli, L. (1989) Time dimension in the geochemical approach and hazard estimates of a volcanic area: the isle of Ischia case (Italy). Journal of Volcanology and Geothermal Research, 36, 327-335.

Simon, J.I., and Reid, M.R. (2005) The pace of rhyolite differentiation and storage in an ‘archetypical’ silicic magma system, Long Valley, California. Earth and Planetary Science Letters, 235, 123– 140.

Slejko, F.F., Petrini, R., Orsi, G., Piochi, M., Forte, C. (2004) Water speciation and Sr isotopic exchange during water-melt interaction: A combined NMR-TIMS study on the Cretaio Tephra (Ischia Island, south Italy). Journal of Volcanology and Geothermal Research, 133, 311-320.

Sneeringer, M., Hart, S. R., Shimizu, N. (1984) Strontium and samarium diffusion in diopside. Geochimica and Cosmochimica Acta, 48, 1589-1608.

Spera, F.J., Bohrson, W.A. (2001) Energy-constrained open-system magmatic processes I: general model and energy-constrained assimilation and fractional crystallization (EC-AFC) formulation. Journal of Petrology, 42, 999-1018.

Stracke, A., Bizimis, M., Salters, V.J.M. (2003) Recycling oceanic crust: quantitative constraints. Geochemistry, Geophysics, Geosystems, 4, 3.

Stroncik, N.A., Klügel, A., Hanstee, T.H. (2009) The magmatic plumbing system beneath El Hierro (Canary Islands): constraints from phenocrysts and naturally quenched basaltic glasses in submarine rock. Contributions to Mineralogy and Petrology, 157, 593.

Thompson, A.B. (1996) Fertility of crustal rocks during anataxis. Transactions of the Royal Society of Edinburgh: Earth Sciences, 87, 1-10.

Always consult and cite the final, published document. See http:/www.minsocam.org or GeoscienceWorld

Tibaldi, A., and Vezzoli, L. (1998) The space problem of caldera resurgence: an example from Ischia Island, Italy. Geologische Roundschau., 87, 53-66.

Tibaldi, A., and Vezzoli, L. (2004) A new type of volcano flank failure: The resurgent caldera sector collapse, Ischia, Italy. Geophysical Research Letters, 31, L14605.

Tibaldi, A. (2015) Structure of volcano plumbing systems: A review of multi-parametric effects. Journal of Volcanology and Geothermal Research, 298, 85-135.

Tomlinson, E.L., Albert, P.G., Wulf, S., Brown, R.J., Smith, V.C., Keller, J., Orsi, G., Bourne, A.J., Menzies, M.A. (2014) Age and geochemistry of tephra layers from Ischia, Italy: constraints from proximal-distal correlations with Lago Grande di Monticchio. Journal of Volcanology and Geothermal Research, 287, 22-39.

Turi, B., and Taylor, H.P. (1976) Oxigen isotope of potassic volcanic rocks of the Roman Province, central Italy. Contribution to Mineralogy and Petrology, 55, 1-31.

Vezzoli, L. Ed. (1988). Island of Ischia. CNR Quaderni de “La ricerca scientifica”, 114-10, p. 126.

Villemant, B., Trigila, R., De Vivo, B. (1993). Geochemistry of Vesuvius volcanics during 1631-1944 period. Journal of Volcanology and Geothermal Research, 58, 291-313.

Washington, H.S. (1906) The Roman Comagmatic Region. 199 p. Carnegie Institution of Washington, Pubblication no. 57.

Willcock, M.A.W., Bargossi, G.M., Weinberg, R.F., Gasparotto, G., Cas, R.A.F., Giordano, G., Marocchi, M. (2015) A complex magma reservoir system for a large volume intra- to extra-caldera ignimbrite: Mineralogical and chemical architecture of the VEI8, Permian Ora ignimbrite (Italy). Journal of Volcanology and Geothermal Research, 306, 17-40.

Always consult and cite the final, published document. See http:/www.minsocam.org or GeoscienceWorld

Figure Captions

Figure 1. Simplified geological map of Ischia showing the outcropping areas of volcanic products of the five eruptive phases (after Orsi et al., 2003; Monti et al., 2010). The III phase has been subdivided in (**a**): Mt. Epomeo Green Tuff outcrop (55 ka paroxysmal event), and (**b**): volcanic products between 55 and 33 ka. White circles represent the samples collected in this study (for details and sample locations see Supplementary Table S1). Inset: schematic map of the four active volcanoes of the Neapolitan District, belonging to the southernmost sector of the Roman Magmatic Province (IS = Ischia, PR = Procida, PF = Phlaegrean Fields, SV = Somma-Vesuvio).

Figure 2. Classification diagram (Le Maitre et al., 1989) of the Ischia volcanic rocks. Solid blue circles and red squares are referred to less- and more-evolved samples with CaO > 2 wt.% (LE) and CaO < 2 wt.% (ME), respectively (see Fig. 3); open red squares represent a sub-group of more evolved samples (H-Sr) with anomalous radiogenic $^{87}Sr/^{86}Sr_i$. (see Fig. 5). Grey circles and squares are literature data and maintain the same subdivision as our samples. Literature data source: Poli et al. (1987, 1989), Vezzoli (1988), Crisci et al. (1989), Civetta et al. (1991), Orsi et al. (1992), Di Girolamo et al. (1995), Piochi et al. (1999), Slejko et al. (2004), D'Antonio et al. (2007, 2013), Andria (2008), Brown et al. (2008, 2014), Melluso et al. (2014).

Figure 3. Harker diagrams of the Ischia volcanic rocks using CaO as differentiation index: (a) K_2O, (b) La, and (c) Sr. The samples plot along similar liquid lines of descent independent on the activity phase in all diagrams. Both K_2O (a) and incompatible trace elements such as La (b) exhibit a marked change of the liquid line of descent from less-evolved to more-evolved samples, whilst compatible trace elements such as Sr (c) define a positive and continuous correlation with CaO with no change of the liquid line of descent. Symbols and data source as in Fig. 2.

Always consult and cite the final, published document. See http:/www.minsocam.org or GeoscienceWorld

Figure 4. (a) Rb *vs.* Sr (bi-log scale), and (b) La/Sm *vs.* V of the Ischia volcanic rocks. The samples exhibit a marked change of the liquid line of descent from less-evolved to more-evolved samples as in the case of CaO (Fig. 2). (a) Sr decreases to <10 ppm, and (b) LREE fractionation has a threefold increase in the more-evolved samples. The temperatures reported in (a) refer to estimates based on mineral-melt equilibria (Brown et al., 2014; Melluso et al., 2014). Symbols and data source as in Fig. 2.

Figure 5. $^{87}Sr/^{86}Sr_i$ *vs.* $^{144}Nd/^{143}Nd$ diagram of the Ischia volcanic rocks compared to other Neapolitan District potassic magmas (PR = Procida, PF = Phlaegrean Fields, SV = Somma-Vesuvio.), along with Tyrrhenian Sea basalts (TS), and Mid-Ocean Ridge basalts (MORB). The overall radiogenic isotope signature of erupted magmas at Ischia has a complete overlap among less- and more-evolved samples. It is noteworthy that the anomalous radiogenic Sr trachytes (H-Sr) have Nd isotope compositions overlapping with other samples. Data source – MORBs: Stracke at al. (2003); mafic Italian volcanic rocks (selected using MgO>3.5 wt%): Turi and Taylor (1976); Baldridge et al. (1981); Peccerillo and Manetti (1985); Joron et al. (1987); Civetta et al. (1991); Caprarelli et al. (1993); Villemant et al. (1993); D'Antonio et al. (1999); Ajuso et al. (1998); Gasperini et al. (2002); Conticelli et al. (2002); Avanzinelli et al. (2008); Melluso et al. (2012). Symbols as in Fig. 2.

Figure 6. (a) CaO, (b) $^{87}Sr/^{86}Sr_i$, and (c) $^{144}Nd/^{143}Nd$ *vs.* age (log scale) diagrams of the erupted magmas at Ischia volcano during the five phase of volcanic activity. Dashed areas represent quiescence periods. (a) The recurrence of less-evolved and more-evolved magmas, using CaO as a *proxy* (see Fig. 3), during the last 150 kyr of volcanic activity, is suggestive of alternating periods of magma chamber recharge and differentiation. (b) The Sr isotope signature of erupted magmas, except the anomalous radiogenic $^{87}Sr/^{86}Sr_i$ samples (H-Sr), has a complete overlap among less- and

Always consult and cite the final, published document. See http:/www.minsocam.org or GeoscienceWorld

more-evolved samples, with a smooth sinusoidal variation curve. (b) The Nd isotope signature of erupted magmas has no clear time dependent variation, and the H-Sr samples have $^{143}Nd/^{144}Nd$ identical to the other more- and less-evolved magmas of the corresponding activity phase. The sample with the most radiogenic Nd and unradiogenic Sr isotope composition is a mafic enclave within the Zaro lava flow. Error bars within symbol size. Symbols and data source as in Fig. 2.

Figure 7. $^{87}Sr/^{86}Sr_i$ *vs.* Sr (log scale) diagram of Ischia volcanic rocks. The two evolution liquid lines of descent represent the EC-AFC (Spera and Bohrson, 2001) model starting from the more-evolved magma (ME) at Sr = 180 ppm during the second step of crystallization (see Table 2 and Supplementary Table S3). The temperature of evolving magmas along the two liquid lines of descent is also reported. Symbols and data source as in Fig. 2

Figure 8. Variation of Sr isotope composition within each activity phase at similar degree of differentiation (i.e., CaO) of the Ischia volcanic rocks. Dashed lines mark the threshold at CaO = 2 wt.% (LE *vs.* ME samples), and $^{87}Sr/^{86}Sr_i = 0.707$ (ME *vs.* H-Sr samples).

Figure 9. $^{87}Sr/^{86}Sr_i$ *vs.* $^{87}Rb/^{86}Sr$ diagram of the Ischia volcanic rocks. Both ME and H-Sr trachytes have high $^{87}Rb/^{86}Sr$ developed during the second step of crystal fractionation (Fig. 4). H-Sr trachytes have also $^{87}Sr/^{86}Sr_i > 0.707$, suggesting a hypothetical ^{87}Sr in-growth process, with an age span from 210 kyr to 1.9 Myr (dashed lines), starting from magmas with nominal $^{87}Sr/^{86}Sr = 0.7065$ (see text). Symbols and data source as in Fig. 2.

Figure 10. $^{87}Sr/^{86}Sr_m$ *vs.* age of samples selected for mineral separation and Rb-Sr isotope dilution analyses with both *anomalous* (a, b), and *normal* (c, d) whole rock $^{87}Sr/^{86}Sr$. Straight lines represent groundmass (gdm) and minerals (san: sanidine, cpx: clinopyroxene) backward evolution of $^{87}Sr/^{86}Sr$

Always consult and cite the final, published document. See http:/www.minsocam.org or GeoscienceWorld

based upon their respective $^{87}Rb/^{86}Sr$. The intersection, i.e. when minerals and groundmass have the same $^{87}Sr/^{86}Sr$, yields the mineral crystallization age. The mineral residence time is then calculated subtracting the K-Ar eruption age (Table 3).

Always consult and cite the final, published document. See http:/www.minsocam.org or GeoscienceWorld

Table Captions

Table 1 – Sr, and Nd isotope composition of the Ischia volcanic rocks

Footnote – errors refer to the least significant digits and represent within-run internal precision at 95% confidence level ($2\sigma_m$). $^{87}Sr/^{86}Sr_i$ is the initial Sr isotope composition calculated at the eruption age.

Table 2 - Energy Constrained Assimilation and Fractional Crystallization model of Ischia trachytes during the second step of crystallization

Footnote – synopsis of the input parameters and results of the EC-AFC model reported exhaustively in supplementary Table S3. The bulk distribution coefficient of Sr (D^{Sr}) during magma evolution has been estimated using (i) the two steps fractionating mineral assemblages identified with major elements by Brown et al. (2014) and Melluso et al. (2014), and (ii) the mineral-melt partition coefficients of Fedele et al. (2009, 2015) on similar rock types from the nearby Phlaegrean Fields. The initial temperature of the magma is from Fig. 4, whilst that of the wall rock is from Brown et al. (2014). The liquidus and solidus temperature of the wall rock, and the bulk distribution coefficient of Sr (D^{Sr}) during wall rock melting (both the Calabrian basement and the GLOSS) has been assumed referring to Thompson (1996).

Table 3 – Rb-Sr isotope dilution and Sr isotope composition of mineral-groundmass pairs of selected Ischia volcanic rocks

Footnote – errors refer to the least significant digits; Rb-Sr age represents mineral-groundmass pair isochron; $^{87}Sr/^{86}Sr_{t0}$ is the Sr isotope composition at the time *t0* of mineral crystallization; K-Ar age represents eruption age; RT is the mineral residence time within the magma chamber; gdm: micro- to crypto-crystalline groundmass, glass: hyaline groundmass, cpx: clinopyroxene, san: sanidine. ISC 10-01 and ISC 10-05 are the *anomalous* $^{87}Sr/^{86}Sr$ trachytes, whilst ISC 10-08 and ISC 10-04

Always consult and cite the final, published document. See http:/www.minsocam.org or GeoscienceWorld

are the *normal* $^{87}Sr/^{86}Sr$ trachytes. Eruption age is from Gillot et al. (1982), Poli et al. (1987), Tibaldi and Vezzoli (2004).

Electronic supplementary material

Table S1 - General petrographic characteristics and sample location of the Ischia volcanic rocks

Footnote - LE: less-evolved samples, ME: more-evolved samples, H-Sr: high radiogenic Sr more-evolved samples. Mineral names: alk-fd = alkali feldspar, pl = plagioclase, bt = biotite, cpx = clinopyroxene, mt = titano-magnetite, ol = olivine, sph = sphene. P.I. = porphyritic index. Vesicularity ranges from 30 to 40 % in pumice and 10% in scoria samples; Groundmass texture varies from micro- to criptocrystalline and hyaline (in pumice). TAS classification: SHO = shoshonite, LT = latite, TR = trachyte, TR/PH = trachyte/phonolite. Volcanic activity phases are from Vezzoli (1988), Orsi et al. (2003), Monti et al. (2010).

Table S2 - Major (wt%, water-free) and trace element (ppm) analyses of the Ischia volcanic rocks

Footnote - K-Ar ages are from Gillot et al. (1982), Poli et al. (1987), Tibaldi & Vezzoli (2004). Volcanic activity phases are from Vezzoli (1988), Orsi et al. (2003), Monti et al. (2010).

Table S3 - Energy Constrained Assimilation and Fractional Crystallization model of Ischia trachytes during the second step of crystallization

Footnote – Input parameters and results of the EC-AFC model (Spera & Bohrson, 2001). The bulk distribution coefficient of Sr and Nd (bulk D0) during magma evolution has been estimated using (i) the two steps fractionating mineral assemblages identified with major elements by Brown et al. (2014) and Melluso et al. (2014), and (ii) the mineral-melt partition coefficients of Fedele et al. (2009, 2015) on similar rock types from the nearby Phlaegrean Fields. The initial temperature of the magma is from Fig. 4, whilst that of the wall rock is from Brown et al. (2014). The liquidus and

Always consult and cite the final, published document. See http:/www.minsocam.org or GeoscienceWorld

solidus temperature of the wall rock, and the bulk distribution coefficients of Sr and Nd (bulk D0) during wall rock melting (both the Calabrian basement and the GLOSS) have been assumed referring to Thompson (1996). The highlighted cells report the evolution of the system up to the equilibration temperature of 750°C, namely: (i) magma temperature (T magma), (ii) magma fraction relative to initial mass of magma body (Mm); (iii) mass of assimilated wall rock relative to initial mass of magma body (Ma), (iv) elemental Sr and Nd, and Sr and Nd isotope composition.

Always consult and cite the final, published document. See http:/www.minsocam.org or GeoscienceWorld

Fig. 1

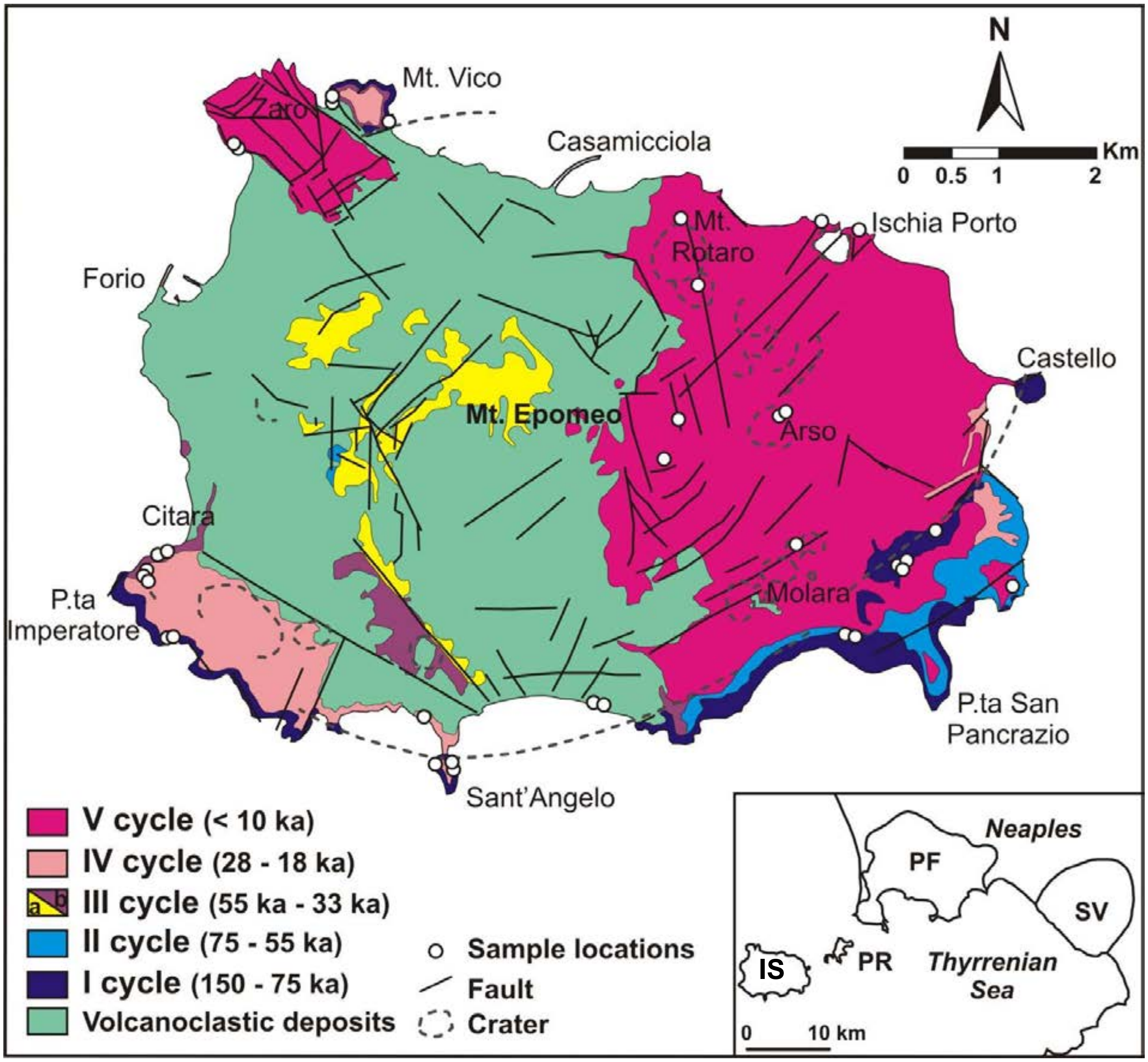
N
Km
0 0.5 1 2
Mt. Vico
Zaro
Casamicciola
Ischia Porto
Mt. Rotaro
Forio
Castello
Mt. Epomeo
Arso
Citara
P.ta Imperatore
Molara
P.ta San Pancrazio
Sant'Angelo
V cycle (< 10 ka)
IV cycle (28 - 18 ka)
III cycle (55 ka - 33 ka)
II cycle (75 - 55 ka)
I cycle (150 - 75 ka)
Volcanoclastic deposits
Sample locations
Fault
Crater
Neaples
PF
SV
IS
PR
Thyrrenian Sea
0 10 km

Fig. 2

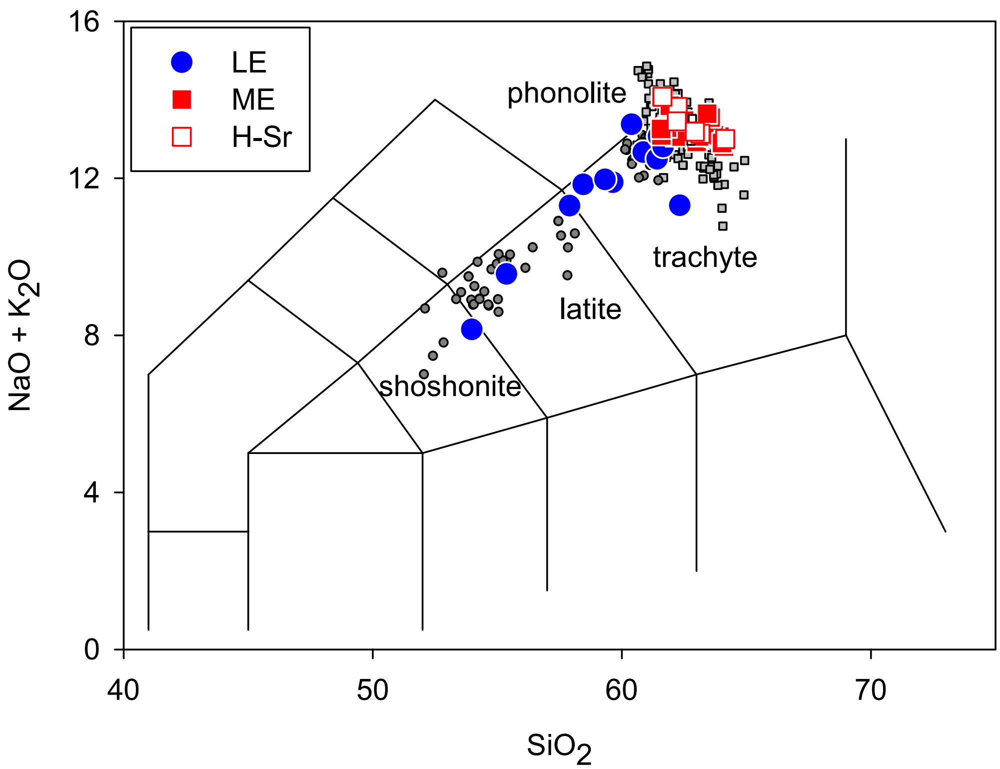
16
12
8
4
0
40
50
60
70
NaO + K2O
SiO2
LE
ME
H-Sr
phonolite
trachyte
latite
shoshonite

This is a preprint, the final version is subject to change, of the American Mineralogist (MSA)
Cite as Authors (Year) Title. American Mineralogist, in press.
(DOI will not work until issue is live.) DOI: http://dx.doi.org/10.2138/am-2017-5724

Fig. 3

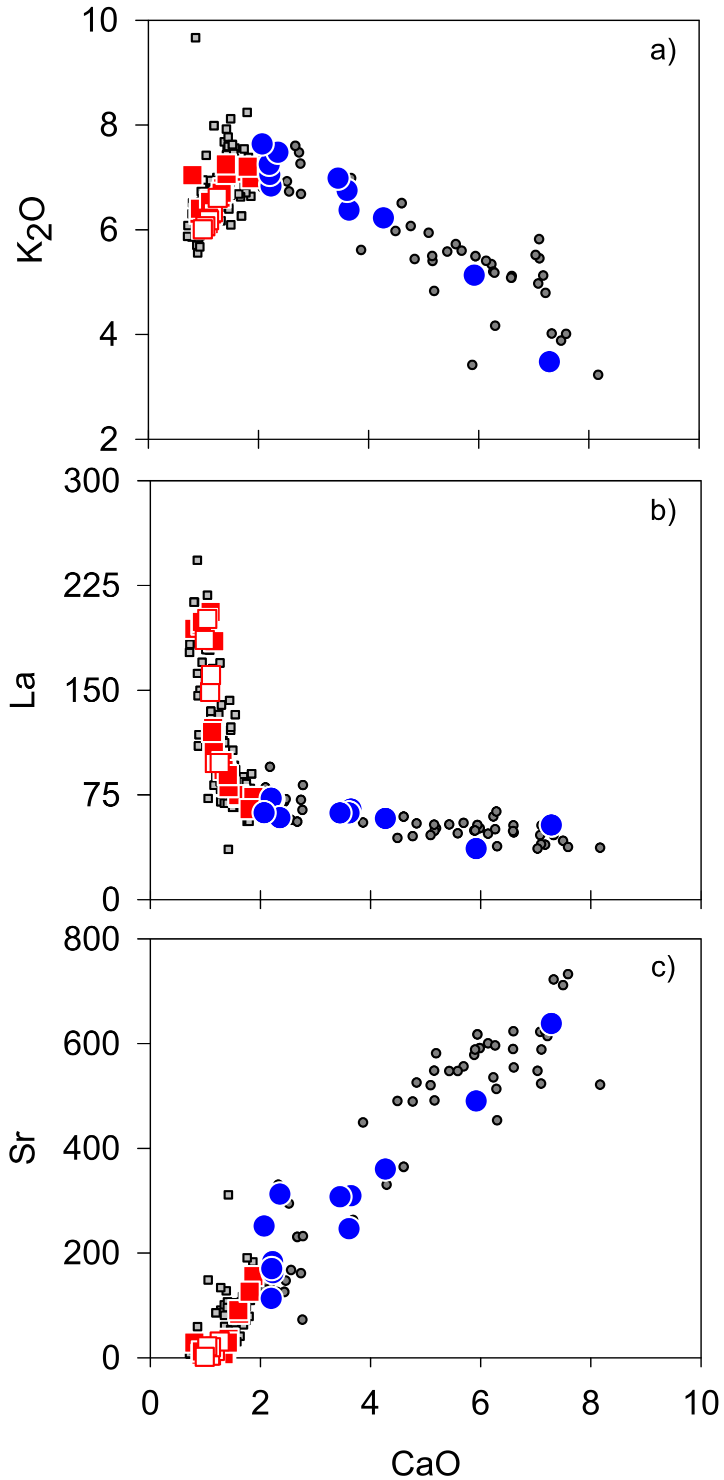

Always consult and cite the final, published document. See http:/www.minsocam.org or GeoscienceWorld

This is a preprint, the final version is subject to change, of the American Mineralogist (MSA)
Cite as Authors (Year) Title. American Mineralogist, in press.
(DOI will not work until issue is live.) DOI: http://dx.doi.org/10.2138/am-2017-5724

Fig. 4

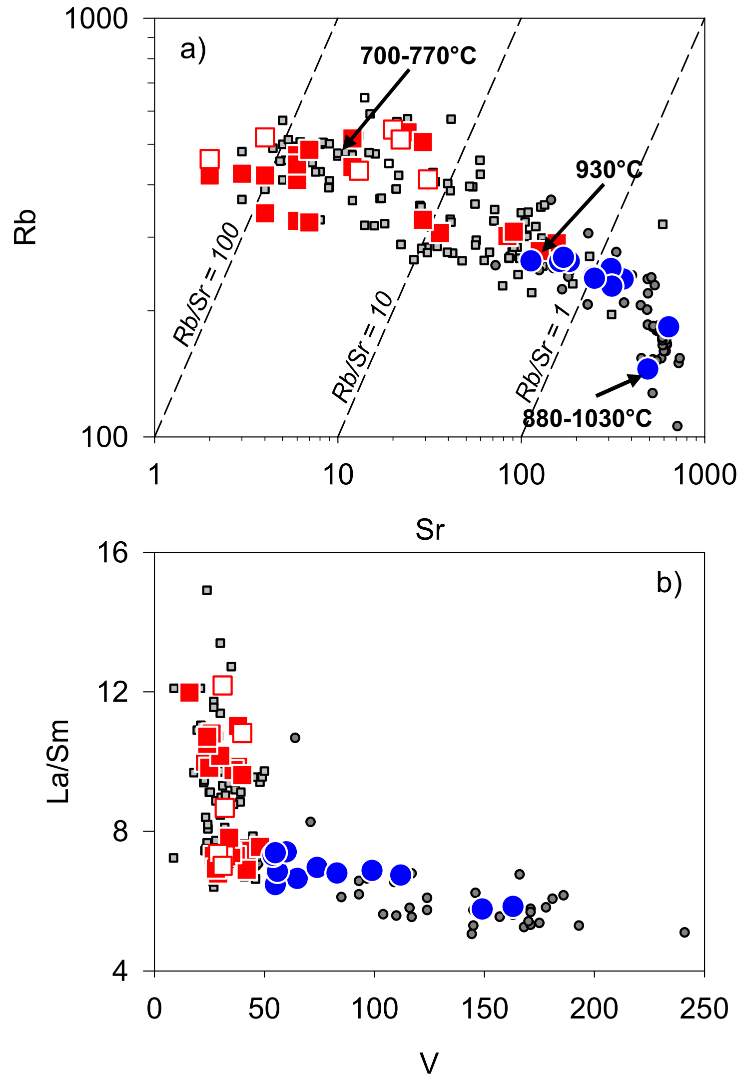

Always consult and cite the final, published document. See http:/www.minsocam.org or GeoscienceWorld

This is a preprint, the final version is subject to change, of the American Mineralogist (MSA)
Cite as Authors (Year) Title. American Mineralogist, in press.
(DOI will not work until issue is live.) DOI: http://dx.doi.org/10.2138/am-2017-5724

Fig. 5

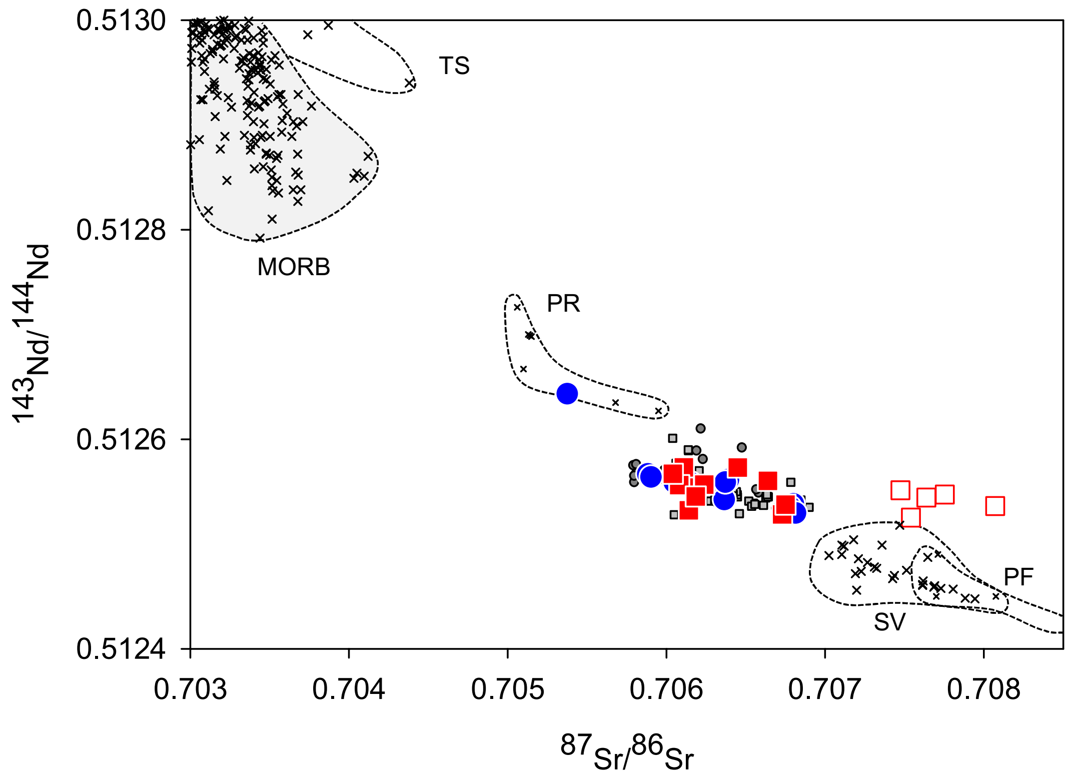

Always consult and cite the final, published document. See http:/www.minsocam.org or GeoscienceWorld

This is a preprint, the final version is subject to change, of the American Mineralogist (MSA)
Cite as Authors (Year) Title. American Mineralogist, in press.
(DOI will not work until issue is live.) DOI: http://dx.doi.org/10.2138/am-2017-5724

Fig. 6

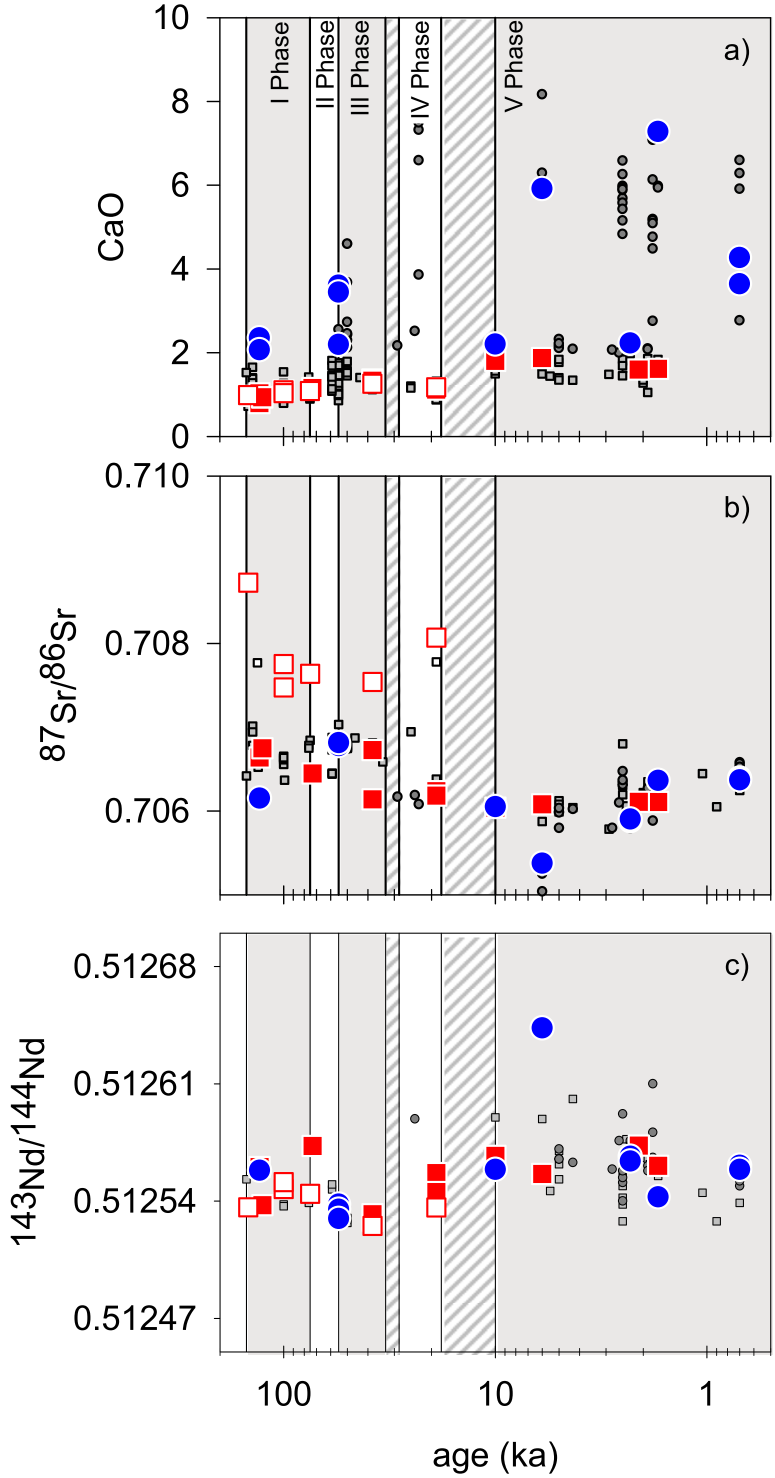

Always consult and cite the final, published document. See http:/www.minsocam.org or GeoscienceWorld

This is a preprint, the final version is subject to change, of the American Mineralogist (MSA)
Cite as Authors (Year) Title. American Mineralogist, in press.
(DOI will not work until issue is live.) DOI: http://dx.doi.org/10.2138/am-2017-5724

Fig. 7

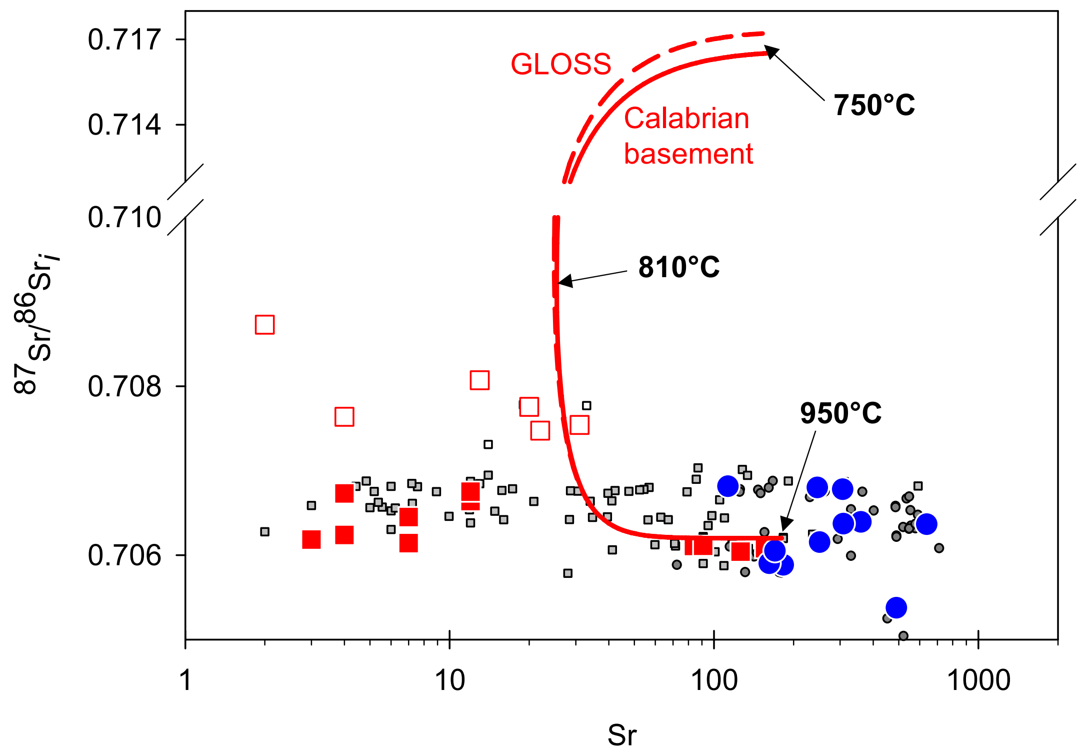

Always consult and cite the final, published document. See http:/www.minsocam.org or GeoscienceWorld

Fig. 8

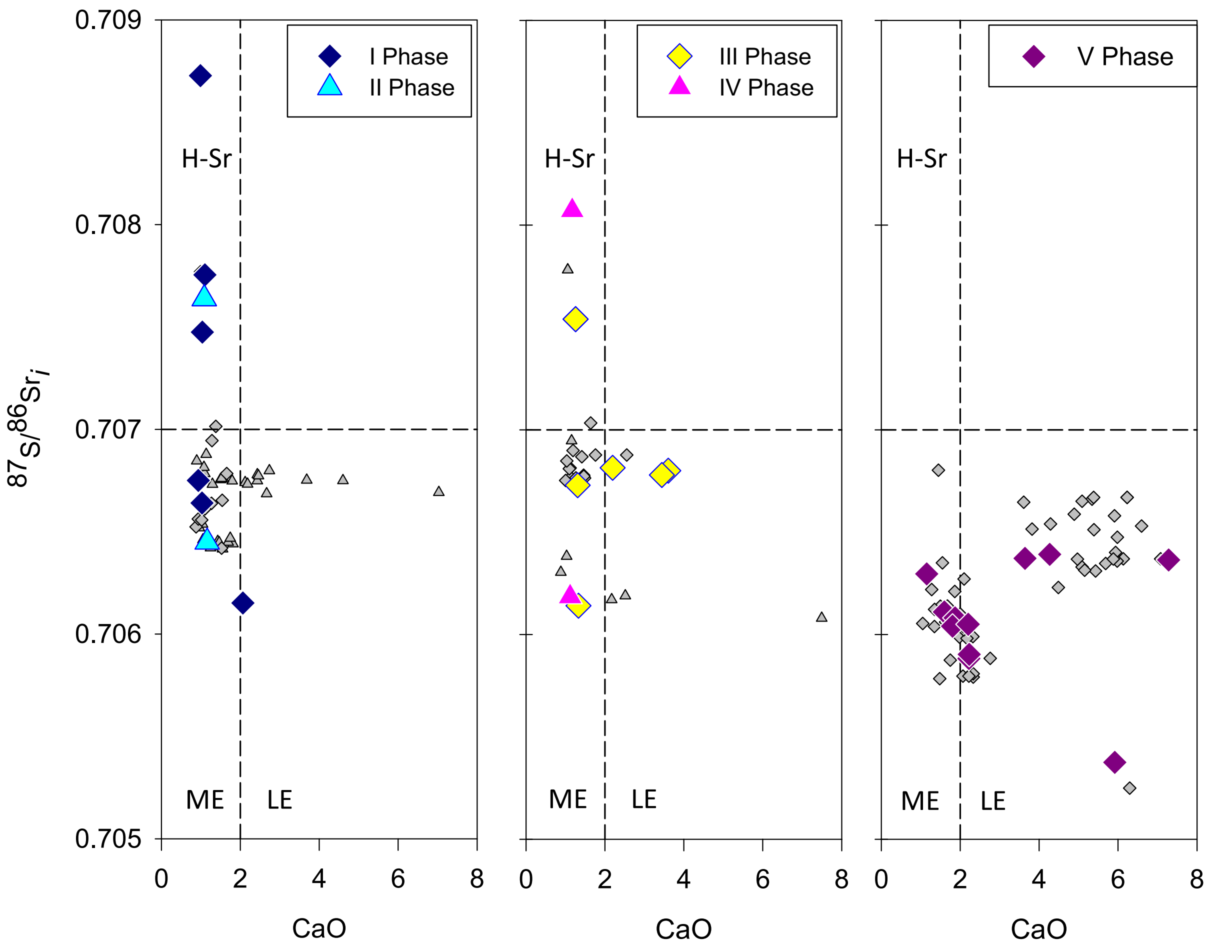
0.709
0.708
0.707
0.706
0.705
$^{87}S/^{86}Sr_i$
I Phase
II Phase
III Phase
IV Phase
V Phase
H-Sr
ME
LE
0
2
4
6
8
CaO

Fig. 9

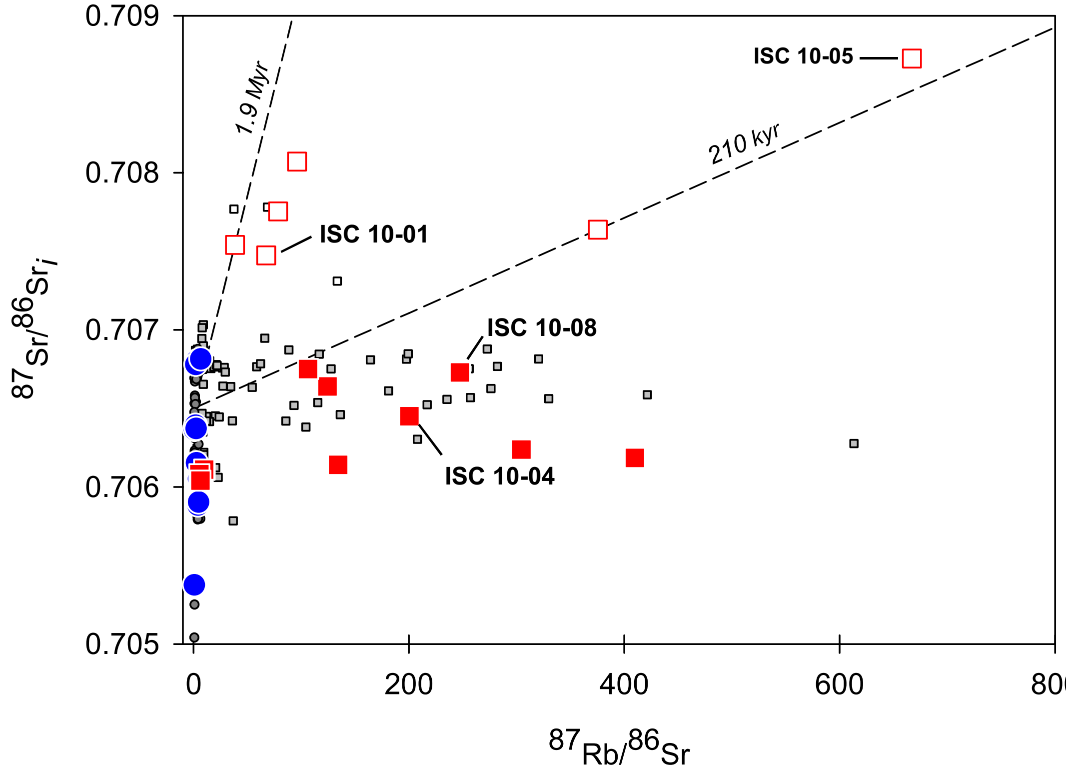
0.709
0.708
0.707
0.706
0.705
0
200
400
600
800
87Sr/86Sri
87Rb/86Sr
1.9 Myr
210 kyr
ISC 10-05
ISC 10-01
ISC 10-08
ISC 10-04

This is a preprint, the final version is subject to change, of the American Mineralogist (MSA)
Cite as Authors (Year) Title. American Mineralogist, in press.
(DOI will not work until issue is live.) DOI: http://dx.doi.org/10.2138/am-2017-5724

Fig. 10

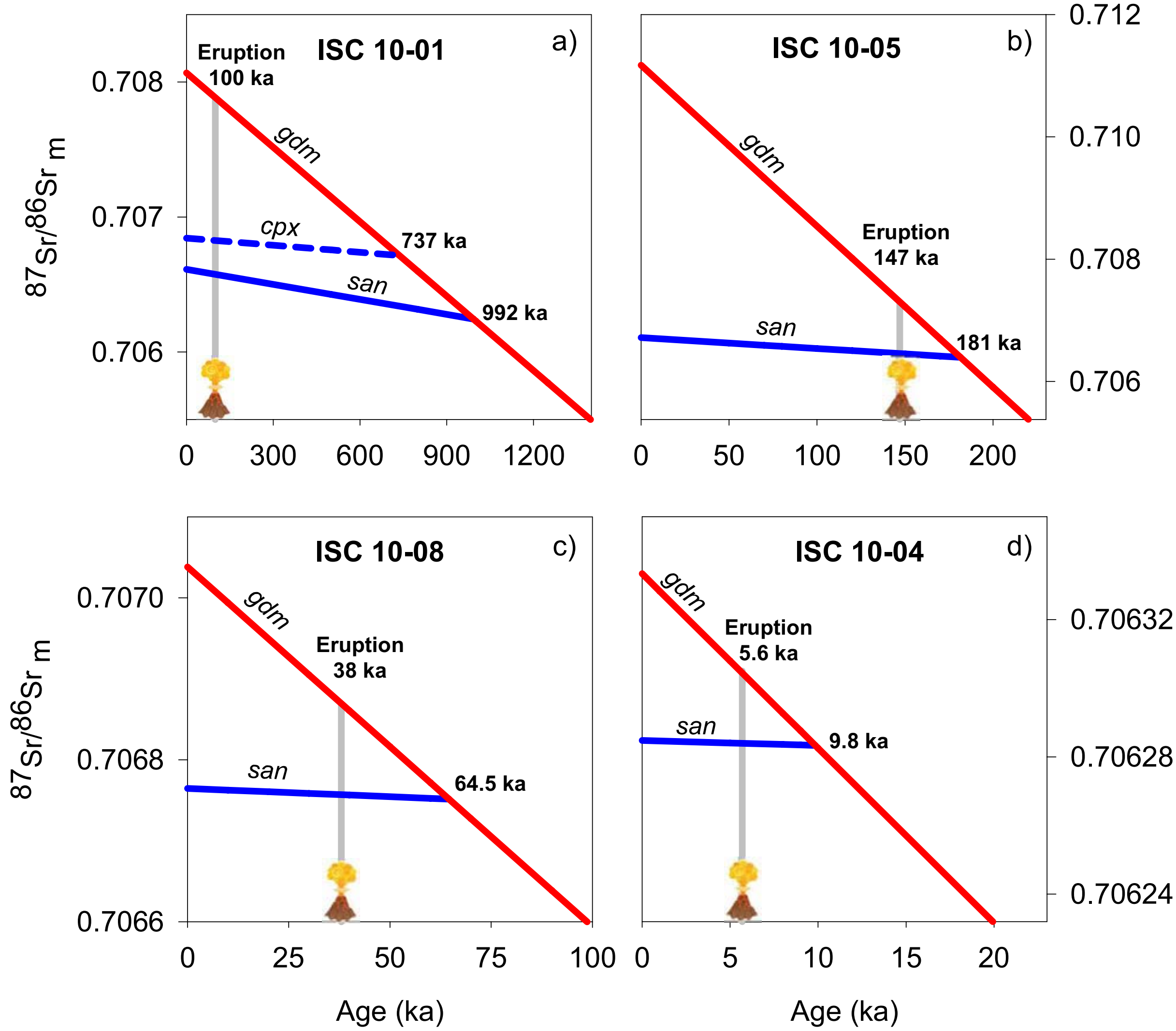

Always consult and cite the final, published document. See http:/www.minsocam.org or GeoscienceWorld

Table 1 – Sr and Nd isotope composition of the Ischia volcanic rocks

Sample	Locality	Phase	age [ka]	$^{87}Rb/^{86}Sr$	$^{87}Sr/^{86}Sr_m$ 2σ_m	$^{87}Sr/^{86}Sr_i$	$^{143}Nd/^{144}Nd$ 2σ_m
ISC 03-01	*Molara Crater*	V	1.7	0.830	0.706364 ± 7	0.70636	0.512542 ± 4
ISC 03-09	*Zaro*	V	6	0.856	0.705375 ± 6	0.70538	0.512643 ± 4
ISC 03-03	*Arso*	V	0.7	1.91	0.706392 ± 7	0.70639	0.512561 ± 5
ISC 03-04	*Arso*	V	0.7	2.36	0.706372 ± 8	0.70637	0.512559 ± 5
ISC 03-06	*Porto d'Ischia*	V	2.3	4.68	0.705903 ± 7	0.70590	0.512564 ± 4
ISC 03-05	*Porto d'Ischia*	V	2.3	4.14	0.705883 ± 6	0.70588	0.512567 ± 5
ISC 03-02	*Cava Bianca*	V	10	6.38	0.706042 ± 7	0.70604	0.512567 ± 4
ISC 03-08	*Zaro*	V	6	5.38	0.706082 ± 7	0.70608	0.512556 ± 5
ISC 03-17	*Mt. Rotaro*	V	2.1	9.82	0.706110 ± 7	0.70611	0.512573 ± 11
ISC 03-07	*Mt. Rotaro*	V	1.7	10.4	0.706109 ± 7	0.70611	0.512561 ± 4
ISC 03-12	*Selva di Napolitano*	V	10	4.56	0.706051 ± 7	0.70605	0.512559 ± 5
ISC 10-04	*St. Angelo*	V	5.6	304	0.706320 ± 5	0.70630	0.512557 ± 4
ISC 03-11	*St. Angelo*	IV	19	96.1	0.708097 ± 7	0.70807	0.512536 ± 5
ISC 10-18	*Pomicione*	IV	19	410	0.706295 ± 7	0.70618	0.512545 ± 4
ISC 03-13b	*Mt. Epomeo*	III	55	2.14	0.706781 ± 7	0.70678	0.512535 ± 5
ISC 03-13a	*Mt. Epomeo*	III	55	2.83	0.706803 ± 7	0.70680	0.512538 ± 5
ISC 03-14	*Mt. Epomeo*	III	55	6.73	0.706819 ± 7	0.70681	0.512530 ± 5
ISC 03-15	*Mt. Vico*	III	38	38.5	0.707561 ± 7	0.70754	0.512525 ± 4
ISC 10-09	*Punta Imperatore*	III	38	134	0.706213 ± 8	0.70614	0.512532 ± 3
ISC 10-08	*Punta Imperatore*	III	38	247	0.706863 ± 7	0.70673	0.512528 ± 5
ISC 03-16	*Mt. Vico*	II	75	375	0.708038 ± 7	0.70764	0.512544 ± 5
ISC 10-16	*Mt. Vico*	II	73	200	0.706658 ± 13	0.70645	0.512573 ± 9
ISC 10-12	*Campagnano*	I	130	124	0.706870 ± 7	0.70664	0.512560 ± 4
ISC 10-14b	*Piano Liguori*	I	130	2.75	0.706157 ± 6	0.70615	0.512558 ± 4
ISC 03-10	*St. Angelo*	I	100	78.4	0.707866 ± 7	0.70775	0.512547 ± 4
ISC 10-01	*St. Angelo*	I	100	67.5	0.707571 ± 6	0.70747	0.512551 ± 4
ISC 10-15b	*Scarrupata di Barano*	I	126	106	0.706941 ± 6	0.70675	0.512538 ± 5
ISC 10-05	*Punta della Signora*	I	147	667	0.710120 ± 26	0.70873	0.512536 ± 5

(DOI will not work until issue is live.) DOI: http://dx.doi.org/10.2138/am-2017-5724

Table 2 - Energy Constrained Assimilation and Fractional Crystallization model of Ischia trachytes during the second step of crystallization

Input parameters

magma liquidus temperature	tlm	970°C	wall rock 1 - Calabrian basement	
initial magma temperature	tm0	950°C	Sr [ppm]	351
wall rock liquidus temperature	tla	900°C	$^{87}Sr/^{86}Sr$	0.7166
initial wall rock temperature	ta0	400°C		
wall rock solidus temperature	ts	650°C	wall rock 2 - GLOSS	
			Sr [ppm]	327
equilibration temperature	Teq	750°C	$^{87}Sr/^{86}Sr$	0.7173
Sr content in magma [ppm]	180		D^{Sr} during wall rock melting	0.8
$^{87}Sr/^{86}Sr$ of magma	0.7062			
D^{Sr} during magma crystallization	3			

Results

Mass fraction and composition of contaminated magma at Teq with:

			wall rock 1	
			Sr [ppm]	160
mass of magma(*)	Mm	0.28	$^{87}Sr/^{86}Sr$	0.7165
mass of assimilated wall rock (*)	Ma	0.22		
(*) normalized to original mass of magma body			**wall rock 2**	
			Sr [ppm]	150
			$^{87}Sr/^{86}Sr$	0.7172

Table 3 – Rb-Sr isotope dilution and Sr isotope composition of mineral-groundmass pairs of selected Ischia volcanic rocks

Sample	phase	Rb [ppm]	2sd	Sr [ppm]	2sd	$^{87}Rb/^{86}Sr$	2 sd	$^{87}Sr/^{86}Sr_m$	$2\sigma_m$	system	$^{87}Sr/^{86}Sr_{t0}$	Rb-Sr age [ka]	K-Ar age [ka]	RT [kyr]
ISC 10-01	gdm	545.1	± 1.3	12.19	± 0.03	129.4	± 0.4	0.708067	± 7					
	cpx	101.4	± 0.2	23.52	± 0.03	12.46	± 0.02	0.706844	± 6	*gdm-cpx*	0.706713	737 ±5.9	100 ±6	637
	san	192.5	± 0.5	21.31	± 0.05	26.13	± 0.10	0.706612	± 14	*gdm-san*	0.706244	992 ±11		892
ISC 10-05	gdm	472.2	± 1.0	0.737	± 0.001	1853	± 5	0.711171	± 6					
	san	184.4	± 0.4	4.26	± 0.01	125.4	± 0.39	0.706718	± 6	*gdm-san*	0.706395	181 ±0.6	147 ±3	34
ISC 10-08	glass	338.4	± 0.7	3.13	± 0.01	312.6	± 0.9	0.707038	± 6					
	san	151.3	± 0.3	30.55	± 0.05	14.33	± 0.04	0.706765	± 6	glass-san	0.706751	65 ±2	38 ±5	27
ISC 10-04	glass	433.7	± 1.0	3.51	± 0.01	358.2	± 1.1	0.706333	± 6					
	san	162.7	± 0.4	46.51	± 0.09	10.12	± 0.03	0.706285	± 6	*glass-san*	0.706283	9.8 ±1.7	5.6 ±0.1	4.2